(1967); S. Ranganathan and M. Nelkin, J. Chem. Phys. 47, 4056 (1967).
[8]M. Nelkin and P. J. Ortoleva, *IAEA Symposium Inelastic Neutron Scattering* (International Atomic Energy Agency, Copenhagen, 1969).
[9]H. B. Callen and T. A. Welton, Phys. Rev. 83, 34 (1951); R. Kubo, Tokyo Summer Lectures in Theoretical Physics, Part 1, Many-Body Theory, 1966 (unpublished).
[10]L. D. Landaue and E. M. Litschitz, *Statistical Physics* (Pergamon, London, 1959).
[11]S. M. Rytov, Zh. Eksperim. i Teor. Fiz. 33, 166 (1957) [Soviet Phys. JETP 6, 130 (1958)].
[12]L. P. Kadonoff and P. C. Martin, Ann. Phys. (N.Y.) 24, 419 (1963).
[13]R. Mountain, Rev. Mod. Phys. 38, 205 (1966).
[14]C. H. Chung and S. Yip, Phys. Rev. 182, 323 (1969).
[15]R. Zwanzig, in *Lectures in Theoretical Physics*, edited by W. E. Brittin, W. B. Downs, and J. Downs (Interscience, New York, 1961), Vol. III.
[16]H. Mori, Progr. Theoret. Phys. (Kyoto) 33, 423 (1965).
[17]H. Mori, Progr. Theoret. Phys. 34, 399 (1965).
[18]A. Z. Akcasu and J. J. Duderstadt, Phys. Rev. 188, 479 (1969).
[19]R. Zwanzig, Phys. Rev. 144, 170 (1966).
[20]M. C. Wang and G. E. Uhlenbeck, Rev. Mod. Phys. 17, 323 (1965); S. Chandrasekhar, *ibid.* 15, 1 (1943).
[21]P. Schofield, Proc. Phys. Soc. (London) 88, 149 (1966).
[22]$\eta_T(k, i\omega)$ will be identified later as the shear viscosity [cf. (4.54)] in an approximate sense.
[23]R. Zwanzig and R. Mountain, J. Chem. Phys. 43, 4464 (1965).

PHYSICAL REVIEW A VOLUME 2, NUMBER 3 SEPTEMBER 1970

Time-Correlation Functions, Memory Functions, and Molecular Dynamics*

G. D. Harp†
Chemistry Department, Brookhaven National Laboratory, Upton, New York 11973
and
Chemistry Department, Columbia University, New York, New York 10027
and
B. J. Berne‡
Chemistry Department, Columbia University, New York, New York 10027
(Received 29 January 1970)

The memory functions for the velocity, angular-momentum, and dipolar autocorrelation functions from a series of molecular-dynamics studies of liquid carbon monoxide are examined. The velocity and angular-momentum memory functions decay initially almost to zero in a Gaussian fashion. However, their long-time behavior has a much slower time dependence. The dipolar memory function from a simulation using a strong noncentral potential is approximately this system's angular-momentum autocorrelation function. Approximate velocity and angular-momentum correlation functions are generated from approximate memory functions and the results are compared to experiment. Gaussian memories based on the second and fourth moments of the corresponding autocorrelation functions give the best agreement with experiment. However, none of the approximate memories examined adequately represents the long-time behavior of the experimental memories. The static atomic radial distribution functions are given and are shown to depend upon the strength of the orientational parts of the pair potential used in the dynamics calculations. The non-Gaussian characteristics of the Van Hove self-correlation functions are examined and shown to depend on the potential and number of particles used in the dynamics calculations. The intermediate scattering function and its memory are also examined.

I. INTRODUCTION

A number of experimental methods exist for probing the structure and molecular dynamics of liquids. X-ray and neutron-scattering experiments determine the structure factor $S(\vec{K})$ which is related by a Fourier transform to the pair-correlation function of the liquid. Inelastic neutron-scattering experiments determine the dynamic form factor $S(\vec{K}, \omega)$, first introduced by Van Hove.[1] $S(\vec{K}, \omega)$ is related to the transition rate for the liquid system to absorb momentum $\hbar\vec{K}$ and energy $\hbar\omega$ from the thermal neutron beam. Moreover, the dynamic form factor $S(\vec{K}, \omega)$ is the Fourier transform of the correlation function of the number densities at two different space-time points. This same function plays an important role in the

TABLE I. Some common experimental quantities and their time-correlation functions. $\vec{V}$ is the c. m. velocity of a molecule. $\vec{J}$ is the angular momentum of a molecule about its c. m. $\vec{u}$ is a unit vector along the molecular axis. $\vec{R}_n$ is the position of a nucleus of type n.

Experimental measurement	Time-correlation function	Property determined
Self-diffusion coefficient D	$\psi(t) \equiv \langle \vec{V}(0) \cdot \vec{V}(t) \rangle / \langle V^2 \rangle$	$D = \frac{1}{3} \langle V^2 \rangle \int_0^\infty dt\, \psi(t)$
Rotational diffusion coefficient of a rod D_R	$A_J(t) \equiv \langle \vec{J}(0) \cdot \vec{J}(t) \rangle / \langle J^2 \rangle$	$D_R = \frac{1}{2} \langle J^2 \rangle \int_0^\infty dt\, A_J(t)$
Nuclear-spin-rotation relaxation time T_I	$A_J(t) \equiv \langle \vec{J}(0) \cdot \vec{J}(t) \rangle / \langle J^2 \rangle$	$(1/T_I) \propto \int_{-\infty}^{+\infty} dt\, e^{-i\omega_0 t} A_J(t)$
Infrared-absorption vibration-rotation spectra in heteronuclear diatomics, $I_a(\omega)$	$D_1(t) \equiv \langle \vec{u}(0) \cdot \vec{u}(t) \rangle$	$\hat{I}_a(\omega) = (1/2\pi) \int_{-\infty}^{+\infty} dt\, e^{-i(\omega - \omega_0)t} D_1(t)$
Raman-scattering vibration-rotation spectra in heteronuclear diatomics, $I_R(\omega)$	$D_2(t) \equiv \langle P_2(\vec{u}(0) \cdot \vec{u}(t)) \rangle$	$\hat{I}_R(\omega) = (1/2\pi) \int_{-\infty}^{+\infty} dt\, e^{-i(\omega - \omega_0)t} D_2(t)$
Depolarization of fluorescence in rodlike molecules (polymers)	$D_2(t) = \langle P_2(\vec{u}(0) \cdot \vec{u}(t)) \rangle$	$r(t) = \frac{2}{5} D_2(t)$
Incoherent neutron scattering	$F_s(\vec{K}, t) = \langle e^{-i\vec{K} \cdot \vec{R}_n(0)} e^{i\vec{K} \cdot \vec{R}_n(t)} \rangle$	$S_s(\vec{K}, \omega) = (1/2\pi) \int_{-\infty}^{+\infty} dt\, e^{-i\omega t} F_s(\vec{K}, t)$

inelastic scattering of light.[2] An experimental determination of $S(\vec{K}, \omega)$ over a wide range of $\vec{K}$ and ω provides an enormous amount of information about the structure and dynamics of liquids.[3,4]

As is well known by this time, the fluctuation dissipation theorem[5] is the basis for relating linear transport coefficients and spectroscopic line shapes to time-correlation functions. A list of some common experimental quantities and their corresponding time-correlation functions is presented in Table I. At present, the complete time dependence of only a few time-correlation functions has actually been determined.[6] In addition, there has been very modest progress on the theoretical side in computing the exact time dependence of specific time-correlation functions,[7] and this only in the simplest cases.

Digital computers have been employed to cope with the difficulties of the many-body problem involved in computing time-correlation functions. Alder and Wainwright[8] solved the classical equations of motion for a system of hard spheres confined to a specified volume V and thereby determined the structure and dynamics of this very simple model system. More recently, Rahman[9] and, later, Verlet[10] studied in great detail the structure and dynamics of liquid argon in which the atoms were assumed to interact via a Lennard-Jones potential. These results are in excellent agreement with the most recent experimental determinations of liquid argon's structure and dynamics. Moreover, these computer studies show that the motion of argon atoms in the liquid is much more complicated than that assumed in earlier simplified-model calculations.

In this article we report the results of a series of computer studies of diatomic liquids. In particular, we emphasize the structural and dynamical properties of these fluids which have not appeared in previous publications. Moreover, this discussion will be presented, wherever possible, in terms of memory functions. Consequently, Sec. II is concerned with a short discussion of the properties of time-correlation functions and their corresponding memory functions.

II. TIME-CORRELATION AND MEMORY FUNCTIONS

Consider the arbitrary mechanical properties $\alpha(\vec{\Gamma})$ and $\beta(\vec{\Gamma})$, and their scalar product $\langle \alpha | \beta \rangle$, where

$$\langle \alpha | \beta \rangle = \int d\Gamma\, \rho(\vec{\Gamma}) \alpha^*(\vec{\Gamma}) \beta(\vec{\Gamma}) , \tag{1}$$

where $\vec{\Gamma}$ is a point in the phase space of the system under consideration, α^* is the complex conjugate of α, and $\rho(\vec{\Gamma})$ is the equilibrium canonical distribution (other ensembles may be used to define this scalar product). This scalar product satisfies the following conditions: (i) $\langle \alpha | \beta \rangle^* = \langle \beta | \alpha \rangle$; (ii) if $\alpha = c_1 \alpha_1 + c_2 \alpha_2$ where c_1 and c_2 are two arbitrary constants, $\langle \beta | \alpha \rangle = c_1 \langle \beta | \alpha_1 \rangle + c_2 \langle \beta | \alpha_2 \rangle$; (iii) $\langle \alpha | \alpha \rangle \geq 0$, the equality sign pertains only if $\alpha = 0$. From (i) the "norm" of the property α, $\langle \alpha | \alpha \rangle$ is real. A property whose norm is unity is said to be normalized. Two observables are said to be orthogonal if $\langle \alpha | \beta \rangle = 0$.

Consider now the mechanical properties $\hat{U}_1, \ldots, \hat{U}_N$. These properties can be represented by the kets $|U_1\rangle, \ldots, |U_N\rangle$ in a vector space and the corresponding bras $\langle U_1|, \ldots, \langle U_N|$ in dual space. Suppose that $\hat{U}_1, \ldots, \hat{U}_N$ are chosen orthonormal

so that $\langle U_i | U_j \rangle = \delta_{ij}$. Moreover, suppose that these properties average to zero, i.e., $\langle U_i \rangle = 0$. Then the set of kets $|U_1\rangle, \ldots, |U_N\rangle$ can be regarded as basis vectors in a subspace of the vector space corresponding to all mechanical properties or (property space). These properties obey the canonical equations

$$\frac{\partial}{\partial t}\hat{U}_j = i\mathcal{L}\hat{U}_j; \quad i\mathcal{L} = \{\ ,\mathcal{H}\},$$

where $\{,\}$ is the Poisson bracket, $\mathcal{H}$ is the Hamiltonian, and $\mathcal{L}$ is the Liouville operator. In property space this becomes the equation

$$\frac{\partial}{\partial t}|U_j\rangle = i\mathcal{L}|U_j\rangle .$$

The time-correlation function $C_{ij}(t)$ is defined by

$$C_{ij}(t) = \langle U_i | e^{i\mathcal{L}t} | U_j \rangle , \tag{2}$$

and the projection operators $\hat{P}_l$ and $\hat{P}$ are defined by

$$\hat{P}_l = |U_l\rangle\langle U_l| , \quad \hat{P} = \sum_{l=1}^{N} |U_l\rangle\langle U_l| . \tag{3}$$

$\hat{P}_l$ is the projector onto the vector $|U_l\rangle$ and $\hat{P}$ is the projector onto the subspace $|U_1\rangle, \ldots, |U_N\rangle$. That these are projectors follows from the fact that they are Hermitian and idempotent, i.e., $\langle \alpha|\hat{P}|\beta\rangle^* = \langle \beta|\hat{P}|\alpha\rangle$ and $\hat{P}^2 = \hat{P}$ (likewise for $\hat{P}_l$).

It is easy to derive an equation for the time evolution of the $N \times N$ matrix $\underline{C}(t)$ with elements $C_{ij}(t)$:

$$\frac{\partial}{\partial t}\underline{C}(t) = i\underline{\Omega}\underline{C}(t) - \int_0^t dt' \underline{K}(t')\underline{C}(t-t') , \tag{4}$$

where $\underline{\Omega}$ is called the frequency matrix and $\underline{K}(t)$ is called the memory-function matrix.

$$K_{ij}(t) = \langle i\mathcal{L}U_i | (1-\hat{P})\, e^{i(1-\hat{P})\mathcal{L}t}(1-\hat{P}) | i\mathcal{L}U_j \rangle ,$$
$$\Omega_{ij} = \langle U_i | \mathcal{L} | U_j \rangle . \tag{5}$$

Generally the properties $|U_i\rangle$ are so chosen that they have definite time-reversal symmetry, that is, they are either even or odd in all the momentum coordinates. In this case $\Omega_{ii} = 0$. A single property $|U_j\rangle$ then[11] satisfies the equation

$$\frac{\partial}{\partial t} C_{jj}(t) = -\int_0^t dt\, K_{jj}(\tau) C_{jj}(t-\tau) ,$$
$$K_{jj}(\tau) = \langle i\mathcal{L}U_j | e^{i(1-\hat{P}_j)\mathcal{L}\tau} | i\mathcal{L}U_j \rangle , \tag{6}$$

where $K_{jj}(t)$ is called the memory function.

It can be shown that $|U_j(t)\rangle$ obeys the exact equations

$$\frac{\partial}{\partial t}|U_j(t)\rangle = -\int_0^t dt\, K_{jj}(t-\tau)|U_j(\tau)\rangle + |F_j(t)\rangle \tag{7}$$

with $|F_j(t)\rangle = e^{i(1-\hat{P}_j)\mathcal{L}t}(1-\hat{P}_j)|i\mathcal{L}U_j\rangle$,

where $|F_j(t)\rangle$ is called a "random force" by analogy with the Langevin equation for the velocity of a Brownian particle. This equation is nevertheless rigorous for the ket $|U_j\rangle$, and moreover, according to its definition, we see that $\langle U_j(0)|F_j(t)\equiv 0$.

Equation (7) was named the "generalized Langevin Equation" by Mori[12] who first derived it. The integral represents a systematic retardation or "frictional effect." It is easy to see from Eq. (7) that

$$K_{jj}(t) = \langle F_j(0)|F_j(t)\rangle = \langle i\mathcal{L}U_j | e^{i(1-\hat{P}_j)\mathcal{L}t} | i\mathcal{L}U_j \rangle , \tag{8}$$

so that the memory function is proportional to the correlation function of the random force. This enables one to construct models for the time evolution of the autocorrelation function based on arguments similar to those used in the "classical" theory of Brownian motion. For example, if it is assumed that the random force has a white spectrum,[13] then $K_{ll}(t) = \lambda\delta(t)$ and the ordinary Langevin equation[13] results with relaxation rate or friction coefficient[11] $\lambda = \int_0^\infty dt K_{ll}(t)$. On the other hand, if the random force is a Gaussian Markov process, according to Doob's theorem,[14] it must have an exponential correlation function so that the memory is exponential, i.e.,

$$K_{ll}(t) = K_{ll}(0)e^{-\lambda t},$$

with $K_{ll}(0) = \langle \dot{U}_l | \dot{U}_l \rangle$. The autocorrelation function will then obey the equation

$$\frac{\partial}{\partial t} C_{ll}(t) = -\langle \dot{U}_l | \dot{U}_l \rangle \int_0^t d\tau e^{-\lambda\tau} C_{ll}(t-\tau). \tag{9}$$

This kind of analysis was first applied with considerable success to the linear-momentum autocorrelation function. It should be noted that $\langle \dot{U}_l | \dot{U}_l |^2 \rangle = \langle |\dot{U}_l|^2 \rangle$ is an equilibrium average. The coefficient λ can be chosen such that $C_{ll}(t)$ gives the correct transport coefficient. Finally, if it is assumed that the autocorrelation function of the random force has a Gaussian dependence on the time, a different, and in many ways more reasonable, result is obtained.

The generalized Langevin equation [Eq. (7)] consequently contributes a great deal to our understanding of the memory-function equation.

Mori[15] has shown that the random force also obeys a generalized Langevin equation, with a random force which obeys yet another Langevin equation. The net result of Mori's analysis is an infinite sequence of Langevin equations in which the dynamical property in the nth equation is the random force of the $(n-1)$th equation. Moreover

the "memory function" $K_n(t)$ in the nth equation is proportional to the autocorrelation function of the random force in the nth equation. Thus,

$$\frac{\partial}{\partial t}|F_n(t)\rangle = -\int_0^t d\tau K_{n+1}(\tau)|F_n(t-\tau)\rangle + |F_{n+1}(t)\rangle, \quad n=0,1,\ldots, \tag{10}$$

where $|F_0(t)\rangle = |U_1(t)\rangle$,

$$K_{n+1}(t) = \langle F_{n+1}(0)|F_{n+1}(t)\rangle / \langle F_n(0)|F_n(0)\rangle,$$

and $\langle F_i(0)|F_j(t)\rangle = \langle F_i(0)|F_i(t)\rangle \delta_{ij}$.

This leads to the continued fraction representation of the Laplace transform of $C_{11}(t)$:

$$\tilde{C}_{11}(s) = 1/s + K_1(0)/s + K_2(0)/s + K_3(0)/\cdots/s + K_m(s) . \tag{11}$$

The quantities $K_n(0)$ are well-defined equilibrium moments. This specific representation is valid only when the property has time-reversal symmetry; otherwise, frequency factors also appear. A sequence of approximations to $C_{11}(t)$ can be arrived at in the following way. Suppose that the autocorrelation function of the random force $|F_m(t)\rangle$ has a white spectrum, i.e., $K_m(t) = \lambda_m \delta(t)$ [where $\lambda_m(t) = \int_0^\infty dt K_m(t)$]. Then $K_m(s) = \lambda_m$ and this assumption truncates the continued fraction and thereby yields a time-correlation function in terms of the equilibrium moments, $K_1(0), \ldots, K_{m-1}(0)$, and the constant λ_m (which can be determined from the known value of the relevant transport coefficient). The following are examples of the above procedure.[15]

(i) Truncation at $|F_2(t)\rangle$; $\tilde{K}_2(s) = \lambda_2$,

$$K_1(0) = \langle \dot{U}_1|\dot{U}_1\rangle ,$$

$$\tilde{C}_{11}(s) = \frac{1}{s + \langle \dot{U}_1|\dot{U}_1\rangle/(s+\lambda_2)} . \tag{12}$$

This result is entirely equivalent to the exponential memory.

(ii) Truncation at $|F_3(t)\rangle$; $\tilde{K}_3(s) = \lambda_3$,

$$K_2(0) = \langle \ddot{U}_1|\ddot{U}_1\rangle / \langle \dot{U}_1|\dot{U}_1\rangle - \langle \dot{U}_1|\dot{U}_1\rangle \equiv \Delta_2^2,$$

$$K_1(0) = \langle \dot{U}_1|\dot{U}_1\rangle , \tag{13}$$

$$\tilde{C}_{11}(s) = 1/s + \langle \dot{U}_1|\dot{U}_1\rangle/s + \Delta_2^2/s + \lambda_3 .$$

This is equivalent to having a memory function

$$\tilde{K}_{11}(s) = \langle \dot{U}_1|\dot{U}_1\rangle/s + \Delta_2^2/s + \lambda_3 . \tag{14}$$

These approximations will be tested against molecular dynamic results in a later section.

The classical autocorrelation function $C_{11}(t)$ and its corresponding memory function $K_{11}(t)$ are real even functions of the time, and can consequently be expanded in an even power series,

$$C_{11}(t) = \sum_{n=0}^{\infty} \frac{(-1)^n}{(2n)!}\gamma_{2n} t^{2n} ,$$
$$K_{11}(t) = \sum_{n=0}^{\infty} \frac{(-1)^n}{(2n)!}\mu_{2n} t^{2n} , \tag{15}$$

where $\gamma_{2n} \equiv \langle (i\mathcal{L})^n U_1 | (i\mathcal{L})^n U_1\rangle = \langle U_1^{(n)}|U_1^{(n)}\rangle$,

$$\mu_{2n} = \langle A_n|A_n\rangle , \tag{16}$$

where $|A_n\rangle = [i(1-\hat{P})\mathcal{L}]^n |i\mathcal{L}U_1\rangle$.

It should also be noted that the power spectra of $C_{11}(t)$ and $K_{11}(t)$,

$$G_{11}(\omega) = (1/2\pi)\int_{-\infty}^{+\infty} dt\, e^{-i\omega t} C_{11}(t) ,$$
$$L_{11}(\omega) = (1/2\pi)\int_{-\infty}^{+\infty} dt\, e^{-i\omega t} K_{11}(t) , \tag{17}$$

are even functions of ω and have the additional property that

$$\int_{-\infty}^{+\infty} d\omega\, \omega^{2n} G_{11}(\omega) = \gamma_{2n} ,$$
$$\int_{-\infty}^{+\infty} d\omega\, \omega^{2n} L_{11}(\omega) = \mu_{2n} . \tag{18}$$

These are called sum rules or moments of the frequency spectrum. The first few moments are

$$\gamma_0 = 1 , \qquad \mu_0 = \langle \dot{U}_1|\dot{U}_1\rangle ,$$
$$\gamma_2 = \langle \dot{U}_1|\dot{U}_1\rangle , \qquad \mu_2 = \langle \ddot{U}_1|\ddot{U}_1\rangle - \langle \dot{U}_1|\dot{U}_1\rangle^2 ,$$
$$\gamma_4 = \langle \ddot{U}_1|\ddot{U}_1\rangle , \qquad \mu_4 = \langle U_1^{(3)}|U_1^{(3)}\rangle + \langle \dot{U}_1|\dot{U}_1\rangle^3 \tag{19}$$
$$\gamma_6 = \langle U_1^{(3)}|U_1^{(3)}\rangle , \qquad - 2\langle \ddot{U}_1|\ddot{U}_1\rangle\langle \dot{U}_1|\dot{U}_1\rangle .$$

There is a relation between the moments of G_{11} and L_{11}

$$\mu_0 = \gamma_2 ,$$
$$\mu_2 = \gamma_4 - \gamma_2^2 ,$$
$$\mu_4 = \gamma_6 - 2\gamma_4\gamma_2 + \gamma_2^3 , \tag{20}$$
$$\vdots$$

Note that μ_{2n} depends on γ_{2n+2} and γ's of lower index.

Consider the vectors $|\alpha\rangle$ and $|\beta\rangle$. According to to the Schwartz inequality,

$$|\langle \alpha|\beta\rangle| \leq [\langle \alpha|\alpha\rangle\langle\beta|\beta\rangle]^{1/2} .$$

Let

$$|\alpha\rangle = |\dot{U}_1\rangle , \quad |\beta\rangle = e^{i(1-\hat{P}_1)\mathcal{L}t}|\dot{U}_1\rangle .$$

Then we have

$$|K_{11}(t)| \leq \langle \dot{U}_1|\dot{U}_1\rangle . \tag{21}$$

Thus, the memory function is bounded above and

below by its initial value.

A complex function of the time $C(t)$ is called positive definite if and only if

$$\sum_{j,k=1}^{n} z_j C(t_j - t_k) z_k^* \geq 0$$

holds for every choice of the finitely many real numbers $t_1, \ldots, t_n$ and complex numbers $z_1, \ldots, z_n$.

According to Bochner's theorem, [16] a continuous function $F(t)$ is the characteristic function of a probability distribution $W(\omega)$, if and only if $F(t)$ is continuous, positive definite, and $F(0)=1$.

Thus if $F(t)$ satisfies the conditions of Bochner's theorem, we have

$$F(t) = \int_{-\infty}^{+\infty} d\omega\, e^{i\omega t} W(\omega) ,$$

where $W(\omega)$ is a probability distribution of the random variable ω.

We have shown elsewhere[17] that the time-correlation function $C_{11}(t)$ and the corresponding normalized memory function $\hat{K}_{11}(t) = K_{11}(t)/K_{11}(0)$ both satisfy the conditions of Bochner's theorem and may thus be regarded as characteristic functions of probability distributions. From Eq. (17) we see by Fourier inversion that

$$\begin{aligned} C_{11}(t) &= \int_{-\infty}^{+\infty} d\omega\, G_{11}(\omega)\, e^{i\omega t}, \\ \hat{K}_{11}(t) &= \int_{-\infty}^{+\infty} d\omega\, P_{11}(\omega)\, e^{i\omega t}, \\ P_{11}(\omega) &= L_{11}(\omega)/K_{11}(0) . \end{aligned} \tag{22}$$

Thus we see that the power spectra may be regarded as probability distributions of the random variable ω. Moreover from the sum rules we can find the moments of these distributions in terms of equilibrium averages. From Eqs. (19) and (22) we have

$$\begin{aligned} \langle \omega^{2n} \rangle_G &= \int_{-\infty}^{+\infty} d\omega\, \omega^{2n} G_{11}(\omega) = \gamma_{2n} , \\ \langle \omega^{2n} \rangle_P &= \int_{-\infty}^{+\infty} d\omega\, \omega^{2n} P_{11}(\omega) = \mu_{2n}/\mu_0 . \end{aligned} \tag{23}$$

This theorem also implies that

$$G_{11}(\omega) \geq 0, \quad P_{11}(\omega) \geq 0 \tag{24}$$

and, thus, contains within it the Wiener-Khinchin theorem.

It is often a very complicated problem to compute these power spectra or the corresponding correlation functions. Consequently, functional forms are usually adopted. There nevertheless exists an approximate method for finding $P_{11}(\omega)$, based on information theory. For this purpose we define an information measure or "entropy" measure of the distribution as

$$S[P_{11}(\omega)] = -\int_{-\infty}^{+\infty} d\omega\, P_{11}(\omega) \ln P_{11}(\omega)$$

according to information theory, [18] if a certain set of moments of $P_{11}(\omega)$ are known; then the optimum $P_{11}(\omega)$ is that which maximizes $S[P_{11}(\omega)]$ subject to the moment constraints. Suppose, for example, that we only know the first two moments

$$\langle \omega^0 \rangle = 1 , \quad \langle \omega^2 \rangle = \mu_2/\mu_0 .$$

Then we must find $P_{11}(\omega)$ such that

$$\delta S[P_{11}(\omega)] = -\delta \int_{-\infty}^{+\infty} d\omega\, P_{11}(\omega) \ln P_{11}(\omega) = 0 ,$$

and

$$\delta \int_{-\infty}^{+\infty} d\omega\, P_{11}(\omega) = 0 , \quad \delta \int_{-\infty}^{+\infty} d\omega\, \omega^2 P_{11}(\omega) = 0$$

are satisfied. This problem is trivial to solve using Lagrange multipliers. $P_{11}(\omega)$ turns out to be

$$P_{11}(\omega) = (\mu_0/2\pi\mu_2)^{1/2} e^{-\mu_0 \omega^2/2\mu_2} . \tag{25}$$

On Fourier inversion [see Eq. (22)], we have

$$\begin{aligned} K_{11}(t) &= K_{11}(0)\hat{K}_{11}(t) = \langle \dot{U}_1 | \dot{U}_1 \rangle \\ &\quad \times e^{-(1/2)(\langle \ddot{U}_1 | \dot{U}_1 \rangle / \langle \dot{U}_1 | \dot{U}_1 \rangle - \langle \dot{U}_1 | \dot{U}_1 \rangle) t^2} . \end{aligned} \tag{26}$$

This approximation turns out to be very useful. Higher moments could have been included to give, hopefully, a better approximation to the memory function. Such approximate memory functions are not only useful in determining the detailed behavior of time-correlation functions, but also give approximate transport coefficients in terms of equilibrium moments. For example, let L be a transport coefficient determined by $C_{11}(t)$:

$$L \propto \int_0^{\infty} dt\, C_{11}(t);$$

L can also be written in terms of the memory function, i.e.,

$$L^{-1} \propto \int_0^{\infty} dt\, K_{11}(t) \propto \tfrac{1}{2} P_{11}(\omega = 0) .$$

We see that in the two-moment information-theory approximation,

$$L^{-1} \propto (\mu_0/8\pi\mu_2)^{1/2} .$$

This shows at once the utility and weakness of this approximation. It would be nice if we could use the known transport coefficient in our optimization procedure but we have not yet found a way to do this.

III. EXPERIMENTAL CORRELATION AND MEMORY FUNCTIONS

In Sec. II it was shown that properties like $\vec{V}$, $\vec{J}$, $\vec{\mu}$, and $e^{i\vec{K}\cdot\vec{R}}$ obey generalized Langevin equations. Consequently, if the "random forces" corresponding to each of these properties are assumed to have white spectra it follows that their respective correlation and memory functions defined in Table II are given by:

TABLE II. The dynamical variables $\vec{V}, \vec{J}, \vec{u}$, and $\vec{R}$ are defined in Table I. The variables which appear here for the first time are $\vec{a}$ is the c.m. acceleration, $\dot{\vec{a}}$ is $d\vec{a}/dt$, $\vec{N}$ is the torque about the c.m., $\dot{\vec{N}} = d\vec{N}/dt$, I is the moment of inertia, and $\vec{K}$ is an arbitrary vector.

Time-correlation function	Time expansion of correlation function [Eqs. (15) and (16)]	Time expansion of corresponding memory [Eqs. (15) and (16)]
$\psi(t) = \dfrac{\langle \vec{V}(0)\cdot\vec{V}(t)\rangle}{\langle V^2\rangle}$	$1 - \frac{1}{2}t^2\dfrac{\langle a^2\rangle}{\langle v^2\rangle} + \dfrac{1}{4!}t^4\dfrac{\langle \dot{a}^2\rangle}{\langle v^2\rangle} + \cdots$	$K_\psi(t) = \dfrac{\langle a^2\rangle}{\langle v^2\rangle} + \dfrac{t^2}{2}\left[\left(\dfrac{\langle a^2\rangle}{\langle v^2\rangle}\right)^2 - \dfrac{\langle \dot{a}^2\rangle}{\langle v^2\rangle}\right] + \cdots$
$A_J(t) = \dfrac{\langle \vec{J}(0)\cdot\vec{J}(t)\rangle}{\langle J^2\rangle}$	$1 - \frac{1}{2}t^2\dfrac{\langle N^2\rangle}{\langle J^2\rangle} + \dfrac{1}{4}t^4\dfrac{\langle \dot{N}^2\rangle}{\langle J^2\rangle} + \cdots$	$K_J(t) = \dfrac{\langle N^2\rangle}{\langle J^2\rangle} + \dfrac{t^2}{2}\left[\left(\dfrac{\langle N^2\rangle}{\langle J^2\rangle}\right)^2 - \dfrac{\langle \dot{N}^2\rangle}{\langle J^2\rangle}\right] + \cdots$
$D_1(t) = \langle \vec{u}(0)\cdot\vec{u}(t)\rangle$	$1 - \dfrac{t^2}{2}\dfrac{\langle J^2\rangle}{I^2} + \dfrac{t^4}{4!}\left(\dfrac{\langle J^4\rangle}{I^4} + \dfrac{\langle N^2\rangle}{I^2}\right) + \cdots$	$K_D(t) = \dfrac{\langle J^2\rangle}{I^2} - \dfrac{t^2}{2}\left(\dfrac{\langle J^2\rangle^2}{I^4} + \dfrac{\langle N^2\rangle}{I^2}\right) + \cdots$
$D_2(t) = \langle P_2(\vec{u}(0)\cdot\vec{u}(t))\rangle$	$1 - \dfrac{3t^2}{2}\dfrac{\langle J^2\rangle}{I^2} + \left(\dfrac{\langle J^4\rangle}{2I^4} + \dfrac{\langle N^2\rangle}{8I^2}\right)t^4 + \cdots$	
$F_s(\vec{K}, t) = \langle e^{-i\vec{K}\cdot\vec{R}(0)} \times e^{i\vec{K}\cdot\vec{R}(t)}\rangle$	$1 - K^2\dfrac{\langle v^2\rangle t^2}{3!} + \dfrac{t^4}{3\times 4!}\left(\langle v^2\rangle^2 K^4 + \langle a^2\rangle K^2\right) + \cdots$	$\Phi_K(t) = K^2\dfrac{\langle v^2\rangle}{3} - \dfrac{t^2}{2}\left(\dfrac{2}{9}\langle v^2\rangle^2 K^4 + \dfrac{\langle a^2\rangle}{3}K^2\right) + \cdots$

$$\psi(t) = e^{-\xi t/m}, \qquad K_\psi(t) = (\xi/M)\delta(t),$$

$$A_J(t) = e^{-\xi_R t/I}, \qquad K_J(t) = \xi_R\delta(t),$$

$$D_1(t) = e^{-2D_R t}, \qquad K_D(t) = 2D_R\delta(t),$$

$$D_2(t) = e^{-6D_R t},$$

$$F_S(\vec{K}, t) = e^{-K^2 D t}, \qquad \Phi_K(t) = K^2 D\delta(t),$$

where ξ and ξ_R are the translational and rotational friction coefficients, D_R is the rotational diffusion coefficient, and D is the translational diffusion coefficient. Moreover, ξ, ξ_R, D_R, and D are often related to the hydrodynamic properties of the system through phenomenological relations like Stokes' Law.

In most cases the assumption of a random force with a white spectrum is completely wrong. We already have an indication of this from the short-time expansions in Table II which indicate a t^2 dependence whereas the exponential gives a $|t|$ dependence at short time. Moreover, the molecular-dynamics calculations indicate gross departures from simple exponentials.

In this section we examine the structure of the above time-correlation functions and memories and compare them with the "experimental" results of two molecular-dynamic simulations discussed in the Appendix. In addition, we compare these "experimental" functions with the simple theories presented in Sec. II.

In Table II the explicit short-time expansions of the relevant time-correlation and memory functions are presented. Note that the time dependences of $\psi(t)$ and $A_J(t)$ are determined only by interactions between a molecule and its environment. That is, in the absence of torques and forces these functions are unity for all time and their memories are zero. There is some justification, then, for viewing these particular memory functions as representing a molecule's temporal memory of its interactions. However, in the case of the dipolar autocorrelation function $D_1(t)$, this interpretation is not so readily apparent. That is, both the dipolar autocorrelation function and its memory will decay in the absence of external torques. This decay is only due to the fact that there is a distribution of rotational frequencies ω for each molecule in the gas phase. In particular, we have for a gas of rigid rotors,

$$\langle \vec{u}(0)\cdot\vec{u}(t)\rangle_G = \int_0^\infty dJ\, P(J)\cos[Jt/I],$$

where $P(J)$ is the probability distribution for the magnitude of the angular momentum. The decay of this function as well as the results of the Stockmayer simulation of carbon monoxide is presented in Fig. 1. Note that the gas phase and Stockmayer results are practically identical which indicates that this potential with the small dipole moment of CO is of little importance in rotational relaxation. Note further that for the dipolar correlation function: (a) The coefficient of the t^2 term, KT/I, depends only on the temperature and a molecule's moment of inertia. Therefore, the dipolar correlation functions from both of the simulations should have the same initial curvature. (b) Molecular interactions enter in the t^4 term which is positive. Therefore interactions will delay the decay of the gas-phase function. These points are all illustrated in Figs. 1 and 2. That is, the dipolar correlation functions all have the same initial curvature and the function from the modified Stockmayer simulation which has a substantial angular-dependent potential decays slower than the gas-phase function. The memory functions for the Stockmayer and modified Stockmayer simulations are presented in Fig. 3 as well as the angular-momentum autocorrelation function from this lat-

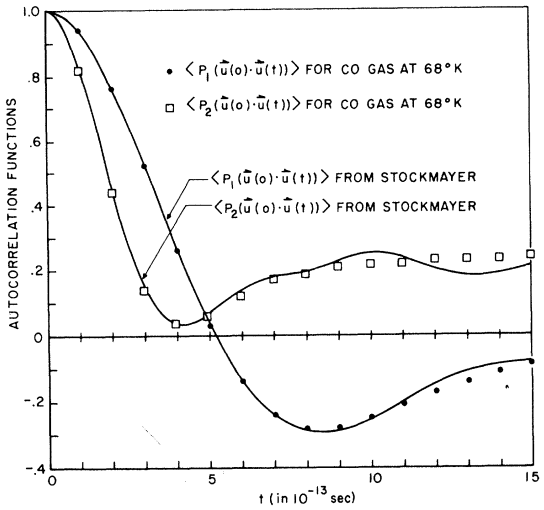

FIG. 1. $\langle \vec{u}(0)\cdot\vec{u}(t)\rangle$ and $\langle P_2\,\vec{u}(0)\cdot\vec{u}(t)\rangle$ in the gas phase and in the liquid phase using the Stockmayer potential.

ter simulation. The memory for the gas-phase or Stockmayer dipolar function decays monotonically and is positive for the $o \leq t \leq 10^{-12}$ sec. On the other hand, the modified Stockmayer memory decays in an entirely different fashion. It goes negative in $\sim 2\times10^{-13}$ sec and is approximately equal to the angular-momentum function for this simulation. This is a very important observation because it presents the possibility of obtaining approximate angular-momentum functions from IR band-shape studies. From Table II we see that the decay of $K_D(t)/K_D(0)$ will be dominated initially at least by molecular interactions, provided $\langle N^2\rangle I^2/\langle J^2\rangle^2 > 1$. This is actually not a difficult criterion to satisfy. In the modified Stockmayer simulation this ratio is ~9.8 and experimentally this ratio is ~4.5 for liquid carbon monoxide at 78 °K. There are probably other physical systems for which this ratio is much larger. In the event that this criterion is

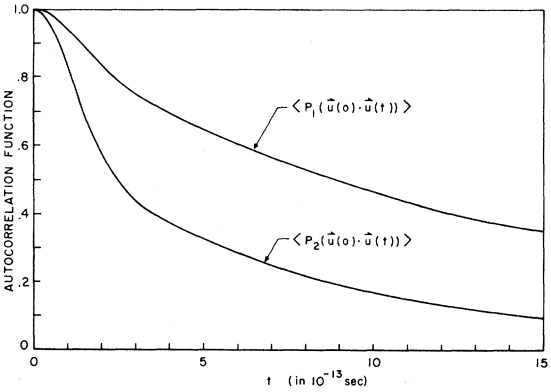

FIG. 2. $\langle \vec{u}(0)\cdot\vec{u}(t)\rangle$ and $\langle P_2(\vec{u}(0)\cdot\vec{u}(t))\rangle$ from the modified Stockmayer simulation.

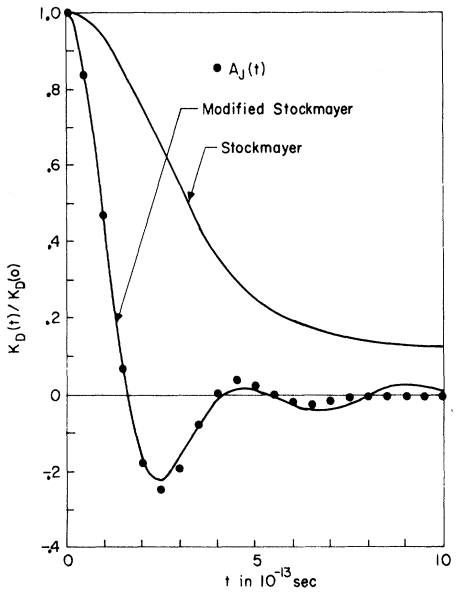

FIG. 3. Memory functions for $\langle \vec{u}(0)\cdot\vec{u}(t)\rangle$ from the Stockmayer and modified Stockmayer simulations. $A_J(t)$ from the modified Stockmayer simulation is also plotted.

satisfied, $K_D(t)/K_D(0) \sim A_J(t)$ to terms in t^2 at least. In the case of the modified Stockmayer simulation we have just seen that this approximation is actually valid throughout the interesting negative region of of $A_J(t)$. Hopefully, this approximation will also be valid in real systems and the interesting negative region of $A_J(t)$ can be verified experimentally from IR band-shape studies by determining $K_D(t)/K_D(0)$.

For completeness consider also the correlation function $D_2(t)$, which can be, and has been, obtained by Fourier inversion of experimental rotation-vibration Raman band shapes.[6] From the short-time expansion of this function (Table II) we see that this function will (a) have a time dependence in the absence of interactions, (b) decay faster initially than $\langle \vec{u}(0)\cdot\vec{u}(t)\rangle$, (c) decay slower in the presence of interactions than in their absence. The gas-phase behavior of this function is given by

$$\langle P_2(\vec{u}(0)\cdot\vec{u}(t))\rangle_G = \tfrac{3}{4}\int_0^\infty \cos(2Jt/I)P(J)\,dJ + \tfrac{1}{4}\,.$$

In the limit $t\to\infty$ the gas-phase function goes to $\frac{1}{4}$, whereas in the limit $t\to\infty$ in a system with interactions $\langle P_2(\vec{u}(0)\cdot\vec{u}(t))\rangle$ goes to zero. These characteristics are all illustrated in Figs. 1 and 2 where the results from the Stockmayer and modified Stockmayer simulations and from a system of gas-phase molecules are presented.

The time-correlation functions have already been discussed from the point of view of the Langevin equation. We saw that the white spectrum probably underestimates the correlations in the

random force since the time-correlation functions are in point of fact nonexponential. At the other extreme we might expect a fluid to have some characteristics of a simple Einstein solid, i.e., a collection of independent oscillators, each oscillating at the same frequency ω_1. The velocity autocorrelation function and its memory would then simply be $\psi(t) = \cos\omega_1 t$, $K_\psi(t) = \omega_1^2$. In this particular instance the memory is a constant, that is, the molecule knows about all its past interactions. We might expect that the actual motion of a fluid particle will have both a diffusive or Brownian character and a solid or vibratory nature. If this were true then the velocity autocorrelation functions should decay in a damped oscillatory fashion. This is indeed the case. All of these studies show clearly that there is an interval of time for which the velocity autocorrelation function is negative (see, for example, Figs. 10 and 12). This behavior is also displayed in Rahman's[9] results for liquid argon and in Alder's[19] results for systems of hard spheres at high densities. This similar behavior is interesting since neither Rahman's nor Alder's systems have internal degrees of freedom while these systems do.

Likewise, all of these studies show clearly that in liquids with potentials that have a strong noncentral character there is an interval of time for which the angular-momentum correlation function is negative (see Fig. 14) whereas in liquids for which the pair potential has a small noncentral character this function remains positive and changes very little over the observed time interval.[20]

Since these autocorrelation functions go negative, the events leading to their decay are correlated. In other words, a molecule must retain some memory of its interactions for a definite time period. This behavior is illustrated in the memory functions for the velocity and angular-momentum autocorrelation functions for the modified Stockmayer simulation, Figs. 6 and 8, and for the velocity autocorrelation function for the Stockmayer simulation, Fig. 4. Note, each of the memories discussed here was calculated using the numerical method outlined elsewhere.[17] All of these memories quickly decay in an approximately Gaussian fashion to almost zero in the time interval $0 \lesssim t \lesssim 3\times10^{-13}$ sec and they all have small positive tails which display much slower time dependences. 3×10^{-13} sec is approximately the average time that it would take a molecule to travel from the center of its cage of nearest neighbors to the "cage wall."

In the following we focus our attention on approximate velocity and angular-momentum autocorrelation functions generated from postulated memory functions. The theory that partially justifies each of these approximations has been outlined in Sec. II. Practically all of the proposed memory functions that we shall consider have already been used by other authors to generate *velocity* autocorrelation functions and/or power spectra which they subsequently compared to Rahman's data. However, it is still informative to examine (a) how well these postulated memories reproduce our experimental memories, and (b) how well the approximate autocorrelation functions generated from these postulated memories reproduce our experimental autocorrelation functions.

The specific memories and their exact functional forms for $K_\psi(t)$ and $K_J(t)$ that we shall consider are as follows.

The exponential memory[21] of Berne *et al.*:

$$K_\psi^*(t) = \frac{\langle a^2\rangle}{\langle v^2\rangle}\exp\left[-t\left(\frac{\langle a^2\rangle}{\langle v^2\rangle}\int_0^\infty \psi(t')\,dt'\right)\right],$$
$$K_J^*(t) = \frac{\langle N^2\rangle}{\langle J^2\rangle}\exp\left[-t\left(\frac{\langle N^2\rangle}{\langle J^2\rangle}\int_0^\infty A_J(t')\,dt'\right)\right], \tag{27}$$

where the asterisks imply that these are postulated memory functions.

(2) Singwi and Tosi's[22] Gaussian memory which is referred to hereafter as Gaussian memory I:

$$K_\psi^*(t) = \frac{\langle a^2\rangle}{\langle v^2\rangle}\exp\left\{-\left[\frac{\pi}{4}t^2\left(\frac{\langle a^2\rangle}{\langle v^2\rangle}\int_0^\infty \psi(t')\,dt'\right)^2\right]\right\},$$
$$K_J^*(t) = \frac{\langle N^2\rangle}{\langle J^2\rangle}\exp\left\{-\left[\frac{\pi}{4}t^2\left(\frac{\langle N^2\rangle}{\langle J^2\rangle}\int_0^\infty A_J(t')\,dt'\right)^2\right]\right\}. \tag{28}$$

(3) The Gaussian memory of Berne[23] and Martin and Yip[24] which is referred to hereafter as Gaussian memory II:

$$K_\psi^*(t) = \frac{\langle a^2\rangle}{\langle v^2\rangle}\exp\left[-\frac{t^2}{2}\left(\frac{\langle \dot a^2\rangle}{\langle a^2\rangle} - \frac{\langle a^2\rangle}{\langle v^2\rangle}\right)\right],$$
$$K_J^*(t) = \frac{\langle N^2\rangle}{\langle J^2\rangle}\exp\left[-\frac{t^2}{2}\left(\frac{\langle \dot N^2\rangle}{\langle N^2\rangle} - \frac{\langle N^2\rangle}{\langle J^2\rangle}\right)\right]. \tag{29}$$

These two memories (a) satisfy the first two moments of the exact memories (see Table II), (b) do not necessarily satisfy the relations

$$\int_0^\infty \psi(t)\,dt = \left[\int_0^\infty K^*(t)\,dt\right]^{-1},$$
$$\int_0^\infty A_J(t)\,dt = \left[\int_0^\infty K_J^*(t)\,dt\right]^{-1},$$

(c) are examples of memory functions whose power spectra are maximal in the information-theory sense when their power spectra are viewed as probability distributions (see the discussion of Bochner's theorem and information theory in Sec. II).

(4) The three-parameter Mori memory:

$$K^*(t) = \frac{\langle a^2\rangle}{\langle v^2\rangle} e^{-\alpha t}\left(\frac{\alpha \sin\Omega t + \Omega\cos\Omega t}{\Omega}\right), \qquad (30)$$

$$K_J^*(t) = \frac{\langle N^2\rangle}{\langle J^2\rangle} e^{-\alpha_J t}\left(\frac{\alpha_J \sin\Omega_J t + \Omega_J \cos\Omega_J t}{\Omega_J}\right),$$

where

$$\alpha = \frac{1}{2}\frac{\langle V^2\rangle}{\langle a^2\rangle}\left(\frac{\langle \dot a^2\rangle}{\langle a^2\rangle} - \frac{\langle a^2\rangle}{\langle v^2\rangle}\right)\left(\int_0^\infty \psi(t)\,dt\right)^{-1},$$

$$\Omega = (\langle \dot a^2\rangle/\langle a^2\rangle - \langle a^2\rangle/\langle v^2\rangle - \alpha^2)^{1/2},$$

$$\alpha_J = \frac{1}{2}\frac{\langle J^2\rangle}{\langle N^2\rangle}\left(\frac{\langle \dot N^2\rangle}{\langle N^2\rangle} - \frac{\langle N^2\rangle}{\langle J^2\rangle}\right)\left(\int_0^\infty A_J(t)\,dt\right)^{-1},$$

$$\Omega_J = (\langle \dot N^2\rangle/\langle N^2\rangle - \langle N^2\rangle/\langle J^2\rangle - \alpha_J^2)^{1/2}.$$

These memories were derived by truncating Mori's continued fraction at $\tilde K_3(s) = \lambda_3$ (see Sec. II). As a consequence, these two memories both satisfy the relations discussed in (a) and (b) of the Gaussian II memories above.

Each of these postulated memories was used to solve the appropriate Volterra equation for the approximate autocorrelation functions $\psi^*(t)$ and $A_J^*(t)$. The specific numerical technique used is discussed elsewhere.[17] Three different experimental autocorrelation functions were tested, the velocity autocorrelation function from both the Stockmayer and modified Stockmayer simulations and the angular-momentum autocorrelation function from the modified Stockmayer simulation. The parameters needed for the postulated memory functions for each of these three autocorrelation functions are tabulated in Table III.

Consider first the postulated and experimental memories displayed in Figs. 4–9. The exponential memories are the poorest approximations to the experimental memories: For short times they decay too rapidly and for long times too slowly. The differences between the short-time behavior of the Gaussian I and the experimental memories are

TABLE III. Data for approximate memory functions.

Simulation	Stockmayer	Modified Stockmayer
$\int_0^\infty \psi(t)\,dt$	1.1503×10^{-13} sec	0.9564×10^{-13} sec
$\int_0^\infty A_J(t)\,dt$		0.5710×10^{-13} sec
$\frac{\langle a^2\rangle}{\langle v^2\rangle}$	$0.6469 \times 10^{26}/\text{sec}^2$	$0.7406\times10^{26}/\text{sec}^2$
$\frac{\langle \dot a^2\rangle}{\langle v^2\rangle}$	$(1.050\pm0.20)\times10^{52}/\text{sec}^4$	$(1.4067\times0.12)\times10^{52}/\text{sec}^4$
$\frac{\langle N^2\rangle}{\langle J^2\rangle}$		$1.2932\times10^{26}/\text{sec}^2$
$\frac{\langle \dot N^2\rangle}{\langle J^2\rangle}$		$(3.3249\pm0.20)\times10^{52}/\text{sec}^4$

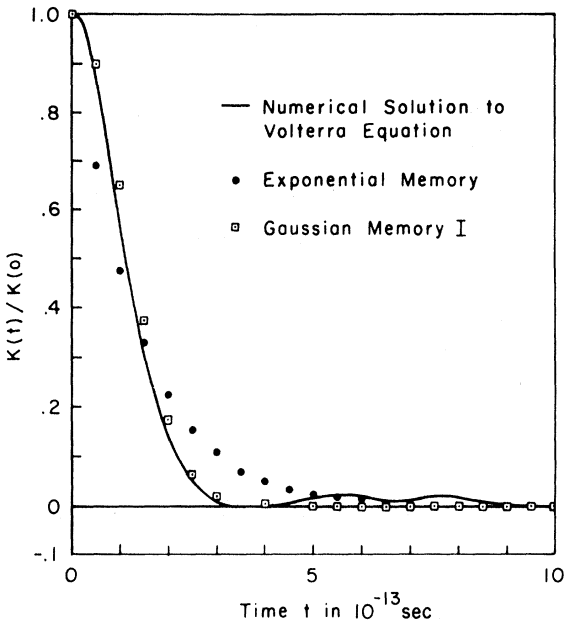

FIG. 4. Memory functions for $\psi(t)$ from the Stockmayer simulation. The approximate memories are the exponential and Gaussian I memories.

quite dependent on the magnitude of the positive tails present in these latter memories: If the tails are large, then the differences are large. To some extent this is also true of the three-parameter Mori memories. Note that these latter memories also go negative near $\sim 3\times10^{-13}$ sec while none of the other memories do. The Gaussian II memories

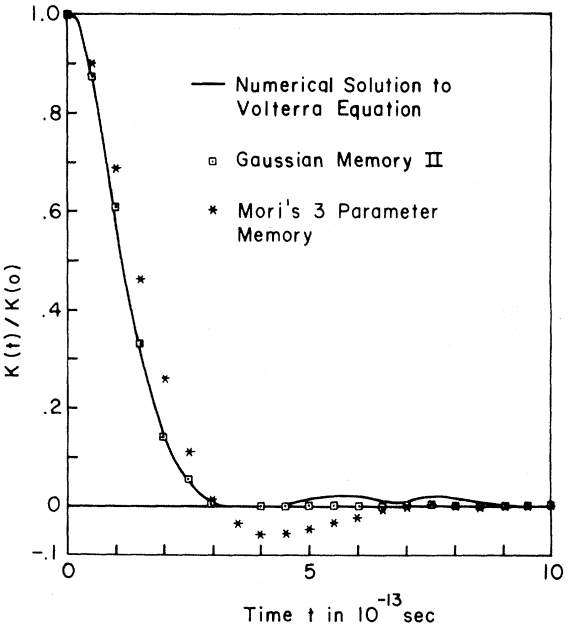

FIG. 5. Memory function for $\psi(t)$ from the Stockmayer simulation. The approximate memories are Gaussian II and Mori's three-parameter memories.

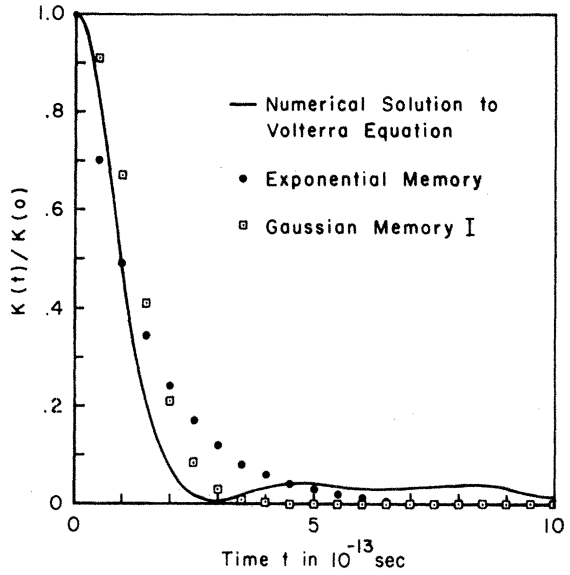

FIG. 6. Memory function for $\psi(t)$ from the modified Stockmayer simulation. The approximate memories are the exponential and Gaussian I memories.

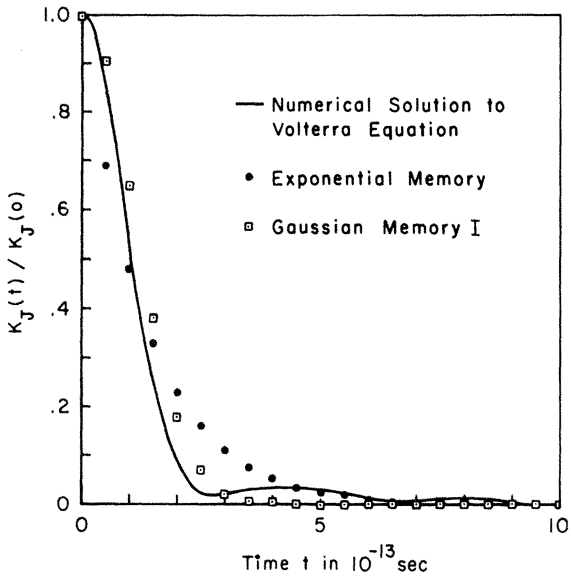

FIG. 8. Memory functions for $A_J(t)$ from the modified Stockmayer simulation. The approximate memories are the exponential and Gaussian I memories.

are excellent approximations to the short-time behavior of the experimental memories. Note further that none of the approximate memories takes into account the presence of the tails in the experimental memories.

Consider next the experimental and approximate autocorrelation functions displayed in Figs. 10–15.

All of the approximate autocorrelation functions are better than the truncated moment expansions in representing the experimental correlation functions (see Table II and Figs. 11, 13, and 15). The Gaussian II autocorrelation functions approximate both the long- and short-time dependences of the experimental autocorrelations better than the functions from either of the other three memory forms.

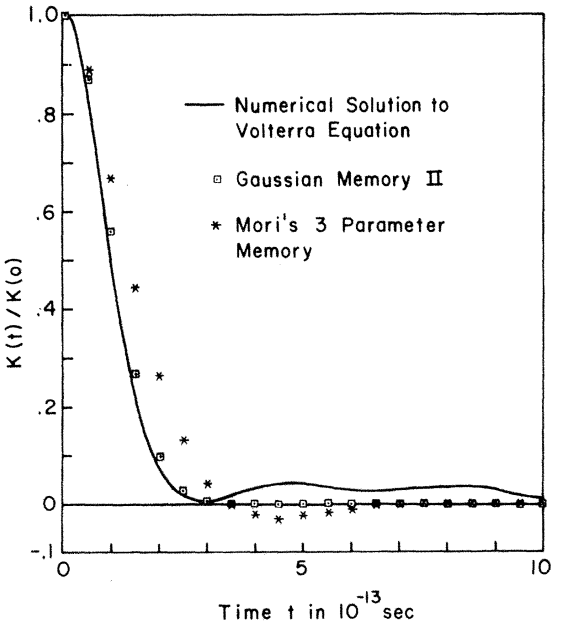

FIG. 7. Memory functions for $\psi(t)$ from the modified Stockmayer simulation. The approximate memories are the Gaussian II and Mori' s three-parameter memories.

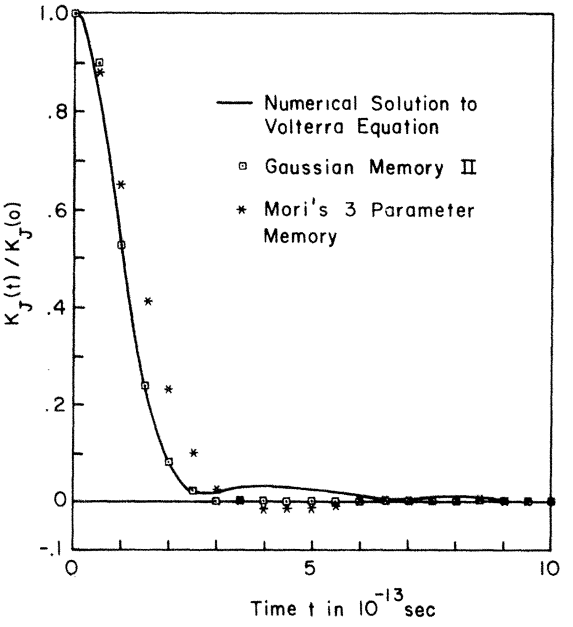

FIG. 9. Memory functions for $A_J(t)$ from the modified Stockmayer simulation. The approximate memories are the Gaussian II and Mori's three-parameter memories.

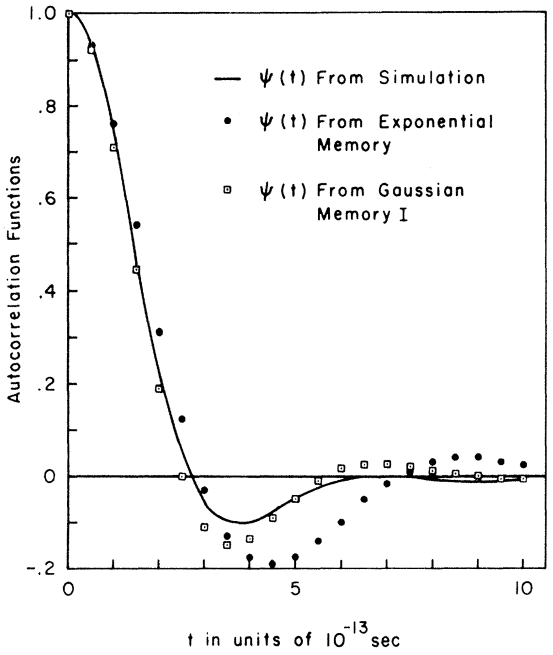

FIG. 10. Approximate velocity autocorrelation functions from the Stockmayer simulation using the exponential and Gaussian I memories.

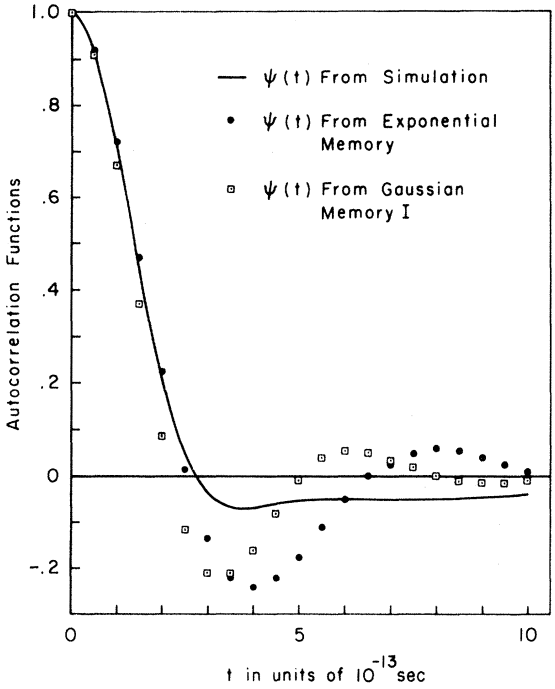

FIG. 12. Approximate velocity autocorrelation functions from the modified Stockmayer simulation using the exponential and Gaussian I memories.

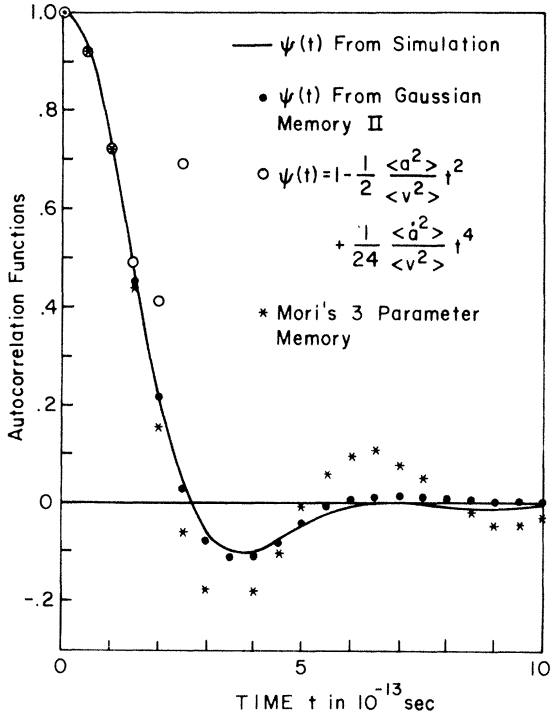

FIG. 11. Approximate velocity autocorrelation functions from the Stockmayer simulation using the truncated moment expansion of $\psi(t)$, and the Gaussian II and Mori's three-parameter memories.

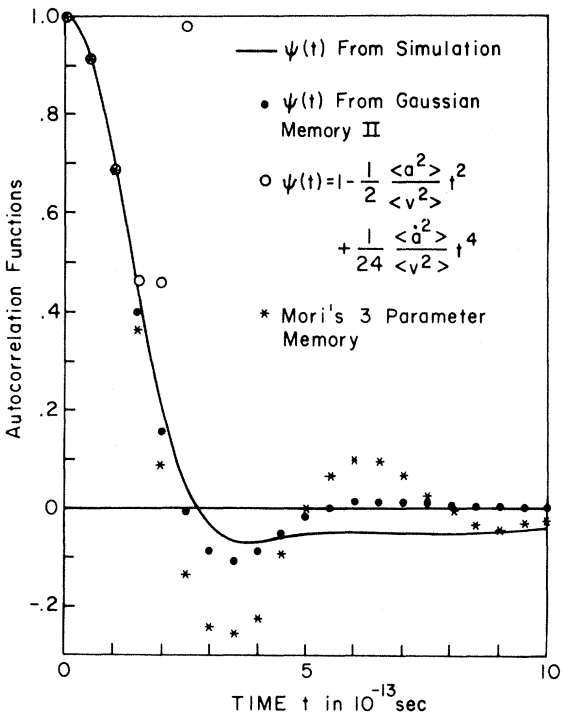

FIG. 13. Approximate velocity autocorrelation functions from the modified Stockmayer simulation using the truncated moment expansion of $\psi(t)$, and the Gaussian II and Mori's three-parameter memories.

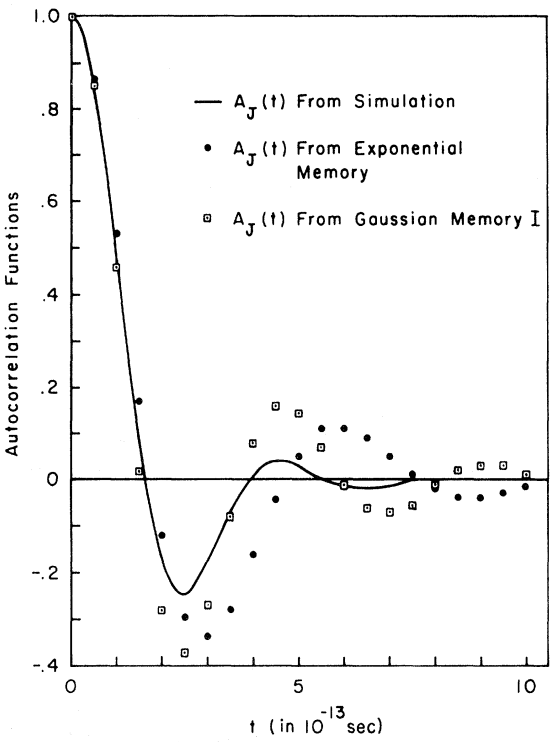

FIG. 14. Approximate angular-momentum autocorrelation function from the modified Stockmayer simulation using the exponential and Gaussian I memories.

By comparing the Gaussian II autocorrelation functions to the experimental ones, we can get some idea of how the tails or long-time behavior of the experimental memories affect their autocorrelation functions. $K_\psi(t)$, from the modified Stockmayer simulation, has the largest tail. From Fig. 13 we see that this tail primarily delays $\psi(t)$'s approach to zero. On the other hand, the tails from the other two experimental memories seem to have very little effect on their correlation functions. This is not quite true when one compares $\int_0^\infty A_J^*(t)\,dt$ and $\int_0^\infty \psi^*(t)\,dt$ for the correlation functions generated from the Gaussian II memories to the appropriate experimental values presented in Table III.

(a) For the Stockmayer simulation we have

$$\int_0^\infty \psi^*(t)\,dt \sim 1.22\times10^{-13}\ \text{sec},$$

while

$$\int_0^\infty \psi(t)\,dt \sim 1.15\times10^{-13}\ \text{sec}.$$

(b) For the modified Stockmayer simulation we have

$$\int_0^\infty \psi^*(t)\,dt \sim 1.16\times10^{-13}\ \text{sec},$$

while

$$\int_0^\infty \psi(t)\,dt \sim 0.96\times10^{-13}\ \text{sec},$$

$$\int_0^\infty A_J^*(t)\,dt \sim 0.70\times10^{-13}\ \text{sec},$$

while

$$\int_0^\infty A_J(t)\,dt \sim 0.57\times10^{-13}\ \text{sec}.$$

In each case the integral of the approximate correlation function is larger than the integral of the experimental function. Also, the difference between the integral of an approximate and the integral of an experimental function is proportional to the magnitude of the long-time behavior of the corresponding experimental memory. In these three examples the neglect of the tail in the experimental memory functions leads to a maximum error of ~23% in the integral of the resulting approximate autocorrelation function.

We conclude the following from the above discussion: (1) The experimental memories for our velocity and angular-momentum autocorrelation functions decay initially to approximately zero in a Gaussian fashion. (2) This initial decay can be adequately approximated by knowing the 2nd and 4th moments of the corresponding autocorrelation functions. (3) The correlation function generated from this approximate memory gives a good approximation to the exact correlation function at least through this latter function's first minimum.

We shall now briefly examine the structure of

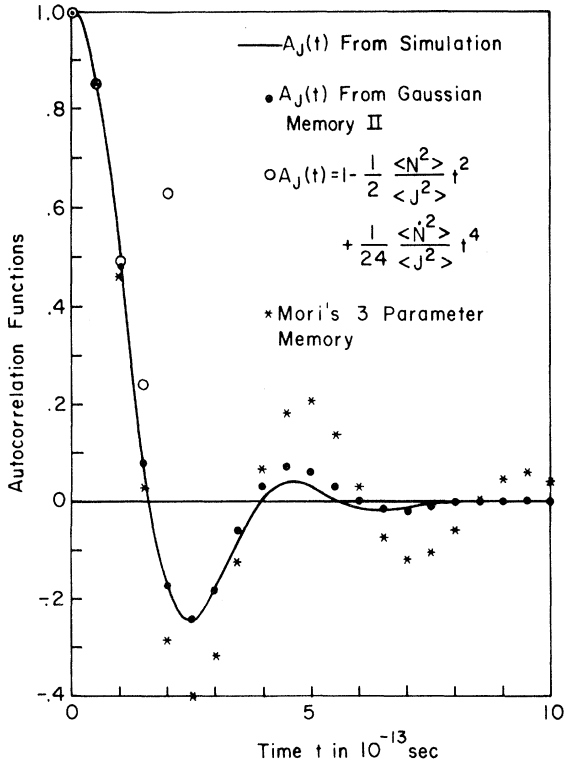

FIG. 15. Approximate angular-momentum autocorrelation from the modified Stockmayer simulation using the truncated moment expansion of $A_J(t)$, and the Gaussian II and Mori's three-parameter memories.

our CO fluids in terms of the four static pair correlation functions $g_{c.m.}(r)$, $g_{C-C}(r)$, $g_{C-O}(r)$, and $g_{O-O}(r)$. These functions are essentially generalizations of the radial distribution function for monatomic fluids and are defined as follows. (1) $g_{c.m}(r)$: Suppose one molecule's c.m. system is located at the origin; then $g_{c.m.}(r)$ is proportional to the probability of finding another molecule's c. m. a distance r away from the first one. (2) $g_{C-C}(r)$: Suppose a carbon atom is located at the origin; then $g_{C-C}(r)$ is proportional to the probability of finding another carbon atom a distance r away. (3) $g_{C-O}(r)$: Suppose a carbon (oxygen) atom is located at the origin; then $g_{C-O}(r)$ is proportional to the probability of finding an oxygen (carbon) atom a distance r away. (4) $g_{O-O}(r)$: Suppose an oxygen atom is located at the origin; then $g_{O-O}(r)$ is proportional to the probability of finding another oxygen atom a distance r away.

These four functions from the Stockmayer and modified Stockmayer simulations of CO are presented in Figs. 16–19. Consider first the c. m. functions. These functions for the two simulations are almost identical and look very much like the radial distribution functions one obtains from x-ray diffraction studies of monatomic liquids such as argon. There is a strong peak at ~3.9 Å which represents the locations of a molecule's first-nearest neighbors. The total number of molecules under this first peak corresponds to ~6 first-nearest neighbors for each molecule. There are also two less intense peaks which represent the locations of a molecule's second- and third-nearest neighbors.

The three atomic-pair correlation functions from the Stockmayer simulations are similar to $g_{c.m.}(r)$

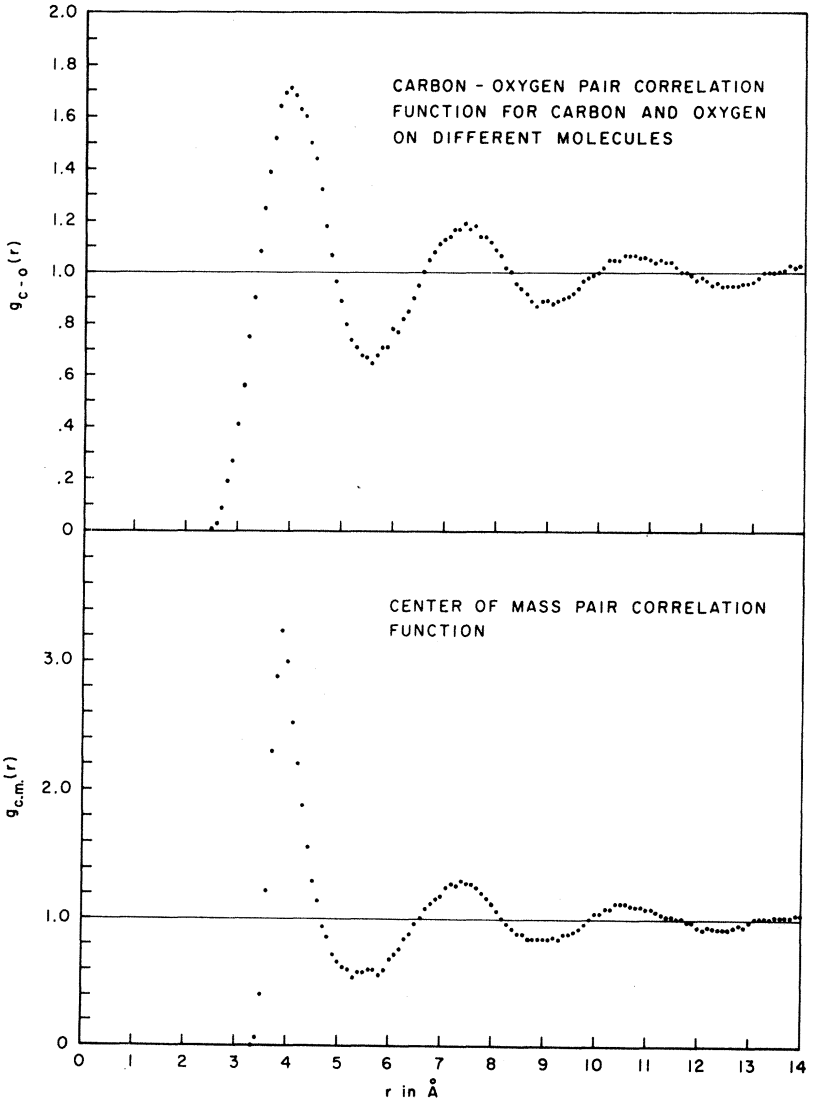

FIG. 16. The c. m. and carbon-oxygen pair-correlation functions from the Stockmayer simulation.

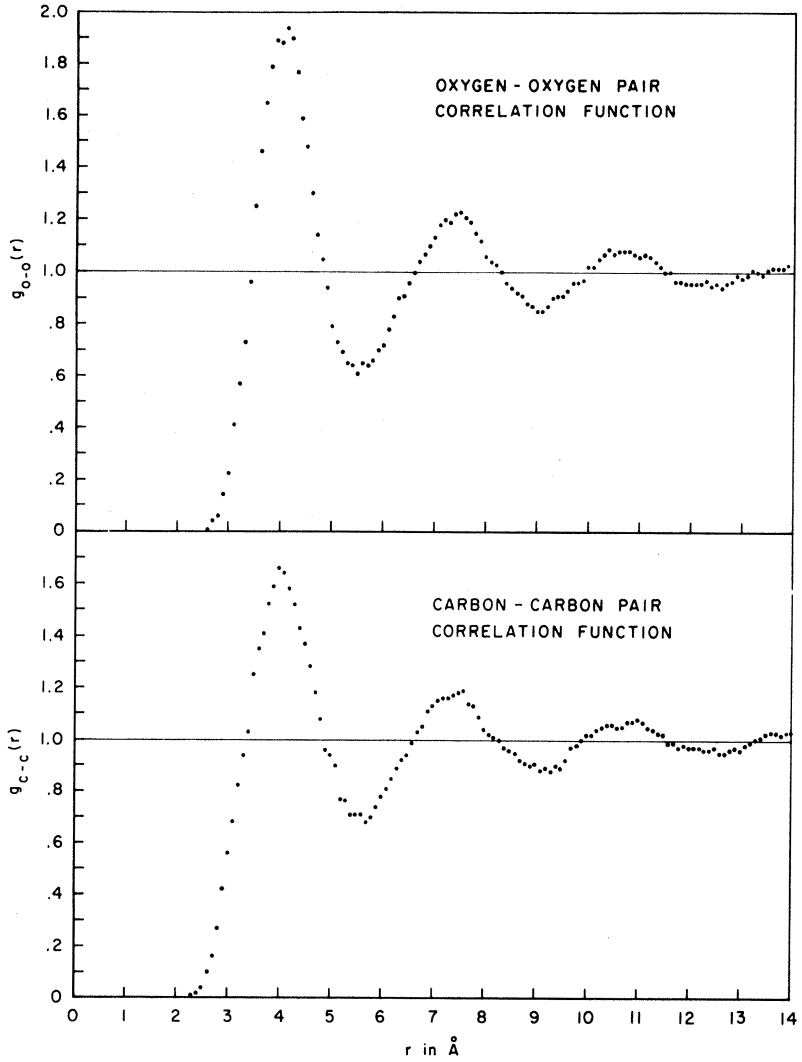

FIG. 17. The oxygen-oxygen and carbon-carbon pair-correlation functions from the Stockmayer simulation.

except that the positions of the first-, second-, and third-nearest neighbors are not so clearly defined; the peaks in the atomic-pair correlation functions are broader and lower than the corresponding peaks in $g_{c.m.}(r)$. Note that the atoms on two different molecules can move closer together than their c.m. . That is, $g_{c.m.}(r)$ is zero for $r \gtrsim 3.2$ Å while $g_{C-C}(r)$ is zero for $r \gtrsim 2.2$ Å. These atomic-pair correlation functions seem to indicate that the CO molecules in the Stockmayer simulation are, on the average, randomly oriented with respect to each other.

The three atomic-pair correlation functions from the modified Stockmayer simulation are similar to the corresponding functions from the Stockmayer simulation except for an asymmetric splitting of the first-nearest-neighbor peak in these former functions. This splitting indicates that, on the average, two molecules which are separated by approximately the first-nearest-neighbor distance are not randomly oriented with respect to each other. That is, there are preferred relative orientations for molecules from this simulation.

One can get a rough estimate of what these preferred orientations are by looking at the most probable orientations for two molecules in the gas phase. There the probability of finding two molecules in a particular orientational configuration $(R, \theta_1, \theta_2, \phi)$ is simply proportional to the Boltzmann factor $\exp[-\beta V(R, \theta_1, \theta_2, \phi)]$, where V is the orientation-dependent potential of interaction between the two molecules. The most probable orientation then corresponds to the minimum of V, V_L, and the least probable corresponds to the maximum of V, V_H. However, if $\beta(V_H - V_L) < 1$, then no particular orientation will be favored and the molecules will be essentially randomly oriented with respect to one another. Suppose we fix R at 3.9 Å, the first-nearest-neighbor distance for the c.m. of two molecules in our liquids, and

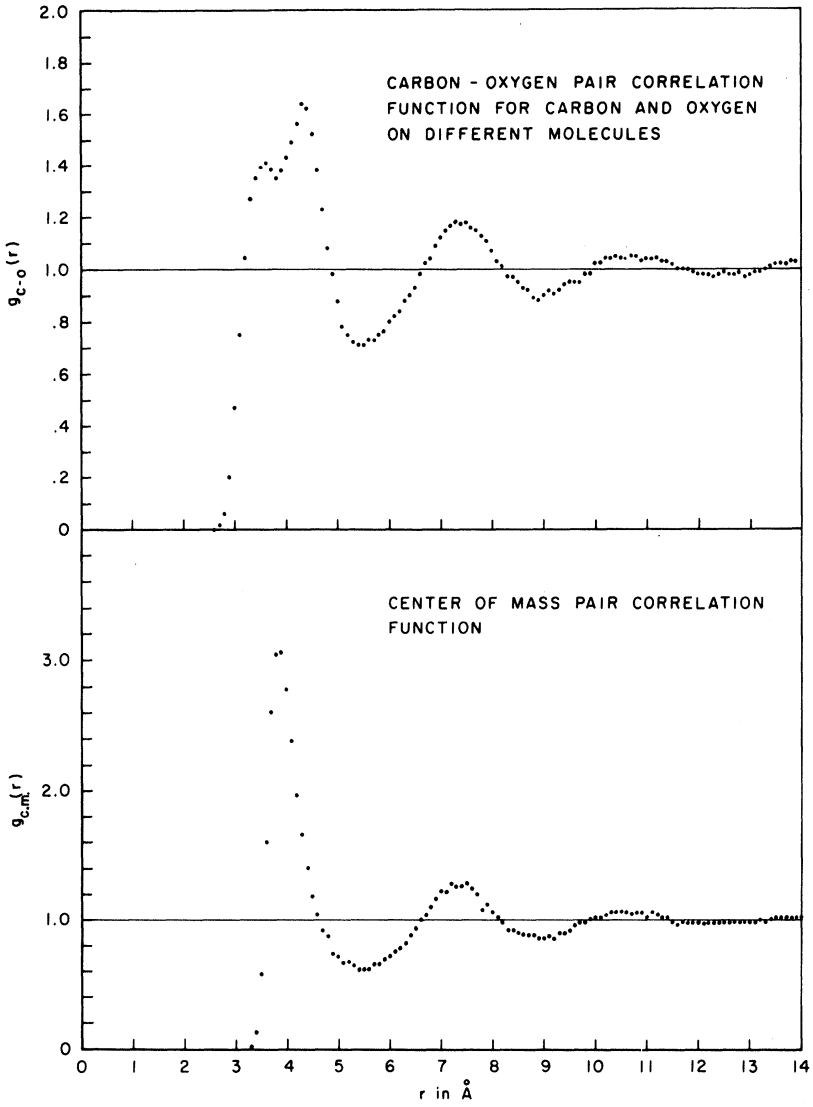

FIG. 18. The c. m. and carbon-oxygen pair-correlation functions from the modified Stockmayer simulation.

look for the maxima and minima of the angular-dependent parts of the Stockmayer and modified Stockmayer potentials. For the dipole-dipole term in the Stockmayer potential we find $V_H = 2\mu^2/R^3$ and $V_L = -2\mu^2/R_3$. For CO at 68 °K, $\beta(V_H - V_L)$ is approximately 0.05. Therefore, this simple analysis predicts that the molecules from this simulation should be essentially randomly oriented with respect to each other.

Suppose we assume that the quadrupole-quadrupole interaction is the dominant term in the angular part of the modified Stockmayer potential. Then for this term we find $V_H = 6Q^2/R^5$ and $V_L = -3Q^2/R^5$. For CO at 68 °K, $\beta(V_H - V_L)$ is approximately 6. Therefore, configurations corresponding to V_L should be favored relative to those corresponding to V_H. There are four equally probable configurations for V_L. If we assume that the most probable distance between the c.m. of two molecules is 3.9 Å and if we assume that the most probable configurations for two molecules are those corresponding to V_L then the atomic-pair correlation functions should have two peaks of the same height in the neighborhood of 3.9 Å: one at ~3.4 Å and one at ~4.4 Å. Therefore, the above simple analysis accounts for the locations of the first two peaks in the atomic-pair correlation functions from the modified Stockmayer simulation but it does not account for their relative intensities.

We shall now discuss the three Van Hove self-correlation functions obtained from our CO simulations. These functions are defined as follows. (1) $G_S(r, t)$ is the probability that the c.m. of a molecule moves a distance r in time t, given that it was at the origin at $t = 0$. (2) $G_S^C(r, t)$ is the probability that the carbon atom on a given mole-

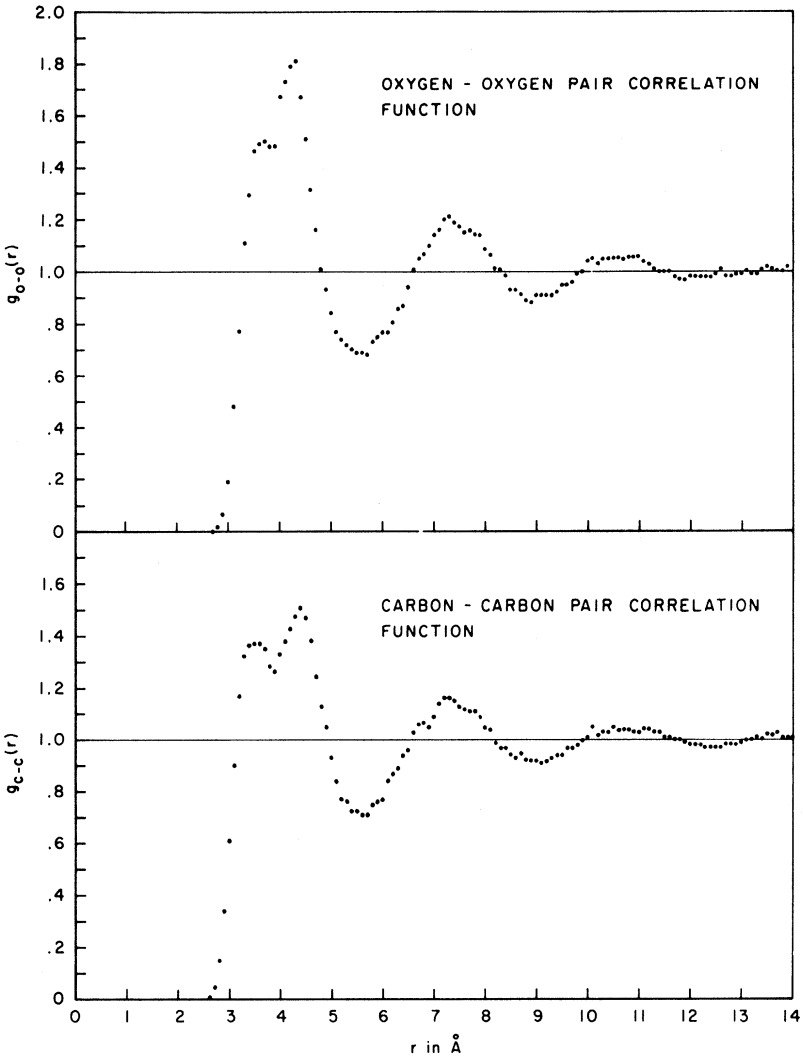

FIG. 19. The oxygen-oxygen and carbon-carbon pair-correlation func- from the modified Stockmayer simulation.

cule moves a distance r in time t, given that it was at the origin at $t=0$. (3) $G_S^O(r,t)$ is the probability that the oxygen atom on a given molecule moves a distance r in time t, given that it was at the origin at $t=0$.

$G_S^O(r,t)$ and $G_S^C(r,t)$ determine the incoherent differential scattering cross section for slow neutrons from CO through a weighted sum of their space-time Fourier transforms. Each of the functions is normalized to unity when integrated over all space, i.e.,

$$4\pi \int_0^\infty G_S(r,t) r^2 dr = 1 \ . \tag{31}$$

The mean-square displacement of the c.m. of an atom or a molecule is given by the second moment of the appropriate self-correlation function. For example, the mean-square displacement of the c.m., $\langle [\Delta \vec{R}_{c.m.}(t)]^2 \rangle$, is given by

$$4\pi \int_0^\infty G_S(r,t) r^4 dr = \langle [\Delta \vec{R}_{c.m.}(t)]^2 \rangle \ , \tag{32}$$

where

$$\Delta \vec{R}_{c.m.}(t) = \vec{R}_{c.m.}(t) - \vec{R}_{c.m.}(0) \ .$$

Suppose we are given the mean-square displacement of the c.m. of an atom or of a molecule. Then, we have shown elsewhere that we can use information theory to develop an approximation for the corresponding Van Hove function. We first defined the information entropy of $G_S(r,t)$, $S[G_S(r,t)]$, as

$$S[G_S(r,t)] = -4\pi \int_0^\infty r^2 G_S(r,t) \ln G_S(r,t) \, dr \ .$$

We then maximized $S[G_S(r,t)]$ subject to the constraints (31) and (32). We found that $G_S(r,t)$ is then given by

$$G_S(r,t) = [\pi W(t)]^{-3/2} \exp[-r^2/W(t)] \ , \tag{33}$$

where

$$W(t) = \tfrac{2}{3} \langle [\Delta \vec{R}_{c.m.}(t)]^2 \rangle \ .$$

This is the well-known Gaussian approximation for $G_S(r,t)$. Vineyard[25] motivated the Gaussian approximation for monatomic systems when he pointed out that $G_S(r,t)$ is a Gaussian for a particle which is moving in a gas, or diffusing according to the simple diffusion equation, or vibrating in an harmonic lattice. Dasannacharya and Rao[26] have determined $G_S(r,t)$ experimentally for liquid argon by Fourier inversion of their incoherent differential scattering cross sections for slow neutrons. They found that, within experimental error, $G_S(r,t)$ is also a Gaussian in liquid argon. Janik and Kowalska[27] have suggested that the Gaussian approximation might also be extended to systems with internal degrees of freedom. However, Rahman's molecular-dynamics studies of liquid argon indicate that $G_S(r,t)$ is not a Gaussian except for short and long times. We also find non-Gaussian corrections to our Van Hove functions, but before discussing these corrections it is informative to examine the Gaussian approximation further.

If one wanted to predict slow-neutron incoherent scattering from CO, then, in the Gaussian approximation, all one would need would be the mean-square displacements of the carbon and oxygen atoms, i.e., $\langle[\Delta\vec{R}_C(t)]^2\rangle$ and $\langle[\Delta\vec{R}_O(t)]^2\rangle$, respectively. These two functions depend in general on both the average translational and rotational behavior of a molecule, as well as translational-rotational coupling. For example, if we express $\vec{R}_C$ and $\vec{R}_O$ in relative and c.m. coordinates then it is easy to show

$$\begin{aligned}\langle[\vec{R}_C(t)]^2\rangle &= \langle[\Delta\vec{R}_{c.m.}(t)]^2\rangle + (2M_O\bar{r}/M)\\ &\quad\times\langle\Delta\vec{R}_{c.m.}(t)\cdot\Delta\vec{\mu}(t)\rangle\\ &\quad+2(M_O\bar{r}/M)^2[1-\langle\vec{\mu}(0)\cdot\vec{\mu}(t)\rangle]\,,\\ \langle[\Delta\vec{R}_O(t)]^2\rangle &= \langle[\Delta\vec{R}_{c.m.}(t)]^2\rangle - (2M_C\bar{r}/M)\\ &\quad\times\langle\Delta\vec{R}_{c.m.}(t)\cdot\Delta\vec{\mu}(t)\rangle\\ &\quad+2(M_C\bar{r}/M)^2[1-\langle\vec{\mu}(0)\cdot\vec{\mu}(t)\rangle]\,,\end{aligned}\tag{34}$$

where $\vec{\mu}$ is a unit vector pointing along the internuclear axis from the oxygen atom to the carbon atom, $\bar{r}$ is the equilibrium internuclear separation, and $\Delta\vec{\mu}(t)=\vec{\mu}(t)-\vec{\mu}(0)$. Note that the atomic displacement functions depend on the dipolar correlation function. Hence, this portion of these functions could be determined by IR band-shape studies. One can prove that

$$\langle[\Delta\vec{R}_{c.m.}(t)]^2\rangle = 2\langle V^2\rangle\int_0^t(t-t')\psi(t')\,dt\,.$$

Therefore, the approximate velocity autocorrelation functions we considered previously could be used to generate $\langle[\Delta\vec{R}_{c.m.}(t)]^2\rangle$. In fact, Berne,[28] Desai and Yip[29] have used the exponential memory to generate the approximate mean-square displacement of an argon atom in the liquid. Desai and Yip[29] then used the Gaussian approximation to predict neutron scattering from liquid argon.

The translational-rotational coupling term $\langle\Delta\vec{R}_{c.m.}(t)\cdot\Delta\vec{\mu}(t)\rangle$ is much more difficult to treat. However, for homonuclear diatomic molecules this term vanishes because of symmetry and for the two systems we studied this term contributed less than either the translational or rotational terms. If we ignore the coupling term, then for short times we have

$$\begin{aligned}\langle[\Delta\vec{R}_{c.m.}(t)]^2\rangle &= \langle V^2\rangle t^2+\cdots\,,\\ \langle[\Delta\vec{R}_C(t)]^2\rangle &= [\langle V^2\rangle+(2KTM_O/MM_C)]t^2+\cdots\,,\\ \langle[\Delta\vec{R}_O(t)]^2\rangle &= [\langle V^2\rangle+(2KTM_C/MM_O)]t^2+\cdots\,.\end{aligned}$$

Since M_O is greater than M_C the displacement of the carbon atom should be initially greater than the displacement of the oxygen atom which in turn should be greater than the displacement of the c.m. Since $1-\langle\vec{\mu}(0)\cdot\vec{\mu}(t)\rangle$ is positive for $t>0$ the above order of displacements should persist for all time, that is, provided the translational-rotational coupling term can be neglected. In the diffusion limit or, equivalently, for long times we have

$$\begin{aligned}\langle[\Delta\vec{R}_{c.m.}(t)]^2\rangle &= 6Dt+C\,,\\ \langle[\Delta\vec{R}_C(t)]^2\rangle &= 6Dt+C+2(M_O\bar{r}/M)^2\,,\\ \langle[\Delta\vec{R}_O(t)]^2\rangle &= 6Dt+C+2(M_C\bar{r}/M)^2\,,\end{aligned}$$

where C is a constant that allows for the fact that a molecule in a fluid is not diffusing initially. Note that for long times the atomic displacements should be parallel to the c.m. displacement provided again that the translational-rotational coupling terms can be neglected. These characteristics are all illustrated in Figs. 20 and 21 where the atomic and c.m. displacement functions from the Stockmayer and modified Stockmayer simulations are presented. The translational-rotational coupling function $2\bar{r}\langle\Delta\vec{R}_{c.m.}(t)\cdot\Delta\vec{\mu}(t)\rangle$ is also presented in these figures. This coupling term is largest for long times in the modified Stockmayer simulation. The translational, rotational, and translational-rotational coupling contributions to the mean-square displacement of a carbon atom in the Stockmayer and modified Stockmayer simulations are presented in Figs. 22 and 23, respectively. The maximum contribution from the coupling term is ~3% in the Stockmayer simulation and ~8% in the modified Stockmayer simulation. Initially, the translational and rotational motions contribute approximately equally to the carbon atom's total displacement. In the modified Stockmayer simulation which represents hindered rotational motion, the

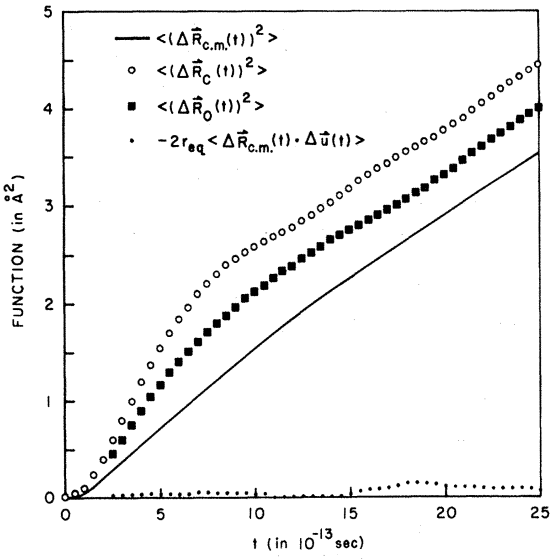

FIG. 20. The atomic displacement functions from the Stockmayer simulation.

translational contribution is larger than the rotational contribution for all times. In fact for $t \gtrsim 10^{-12}$ sec the translational contribution is ~4 times the rotational one. On the other hand, in the Stockmayer simulation which represents free rotational motion there is a region near $t = 5\times10^{-13}$ sec where the rotational contribution is larger than the translational one. However, for long times the translational contribution is again larger than the rotational contribution in this simulation.

We shall now discuss the non-Gaussian behavior of our self-correlation functions. Rahman[9] pointed out that it is convenient to do this by introducing the coefficients $C_N(t)$ which for $G_S(r,t)$ are defined as

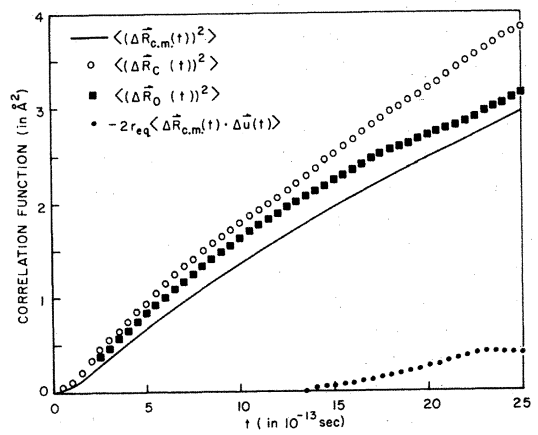

FIG. 21. The atomic displacement functions from the modified Stockmayer simulation.

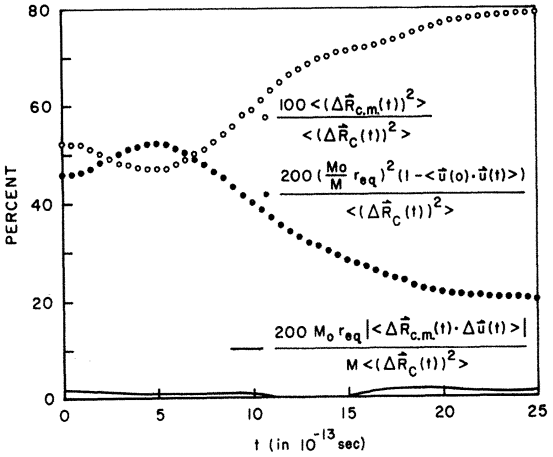

FIG. 22. Percent Contributions to the mean-square displacement of the carbon atom in the Stockmayer simulation.

$$\alpha_N(t) = [\langle[\Delta\vec{R}_{c.m.}(t)]^{2N}\rangle / C_N\langle[\Delta\vec{R}_{c.m.}(t)]^2\rangle^N] - 1,$$

$$N = 2, 3, 4,$$

where C_N is given by

$$C_N = 1\times3\times\cdots\times(2N+1)/3^N.$$

The coefficients for $G_S^O(r,t)$ and $G_S^C(r,t)$ are defined in a similar manner. If a self-correlation function is a Gaussian then the corresponding coefficients $\alpha_N(t)$ will vanish. For example, for short times we have

$$\langle[\Delta\vec{R}_{c.m.}(t)]^{2N}\rangle = \langle V^{2N}\rangle t^{2N}, \quad \langle V^{2N}\rangle = C_N\langle V^2\rangle^N.$$

Therefore, for short times these coefficients for $G_S(r,t)$ should vanish.

These coefficients are strongly dependent on the number of molecules used in the simulations. For example, Figs. 24 and 25 present the coefficients

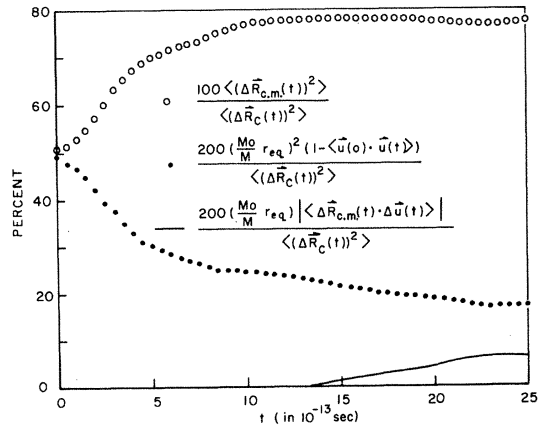

FIG. 23. Percent contributions to the mean-square displacement of the carbon atom in the modified Stockmayer simulation.

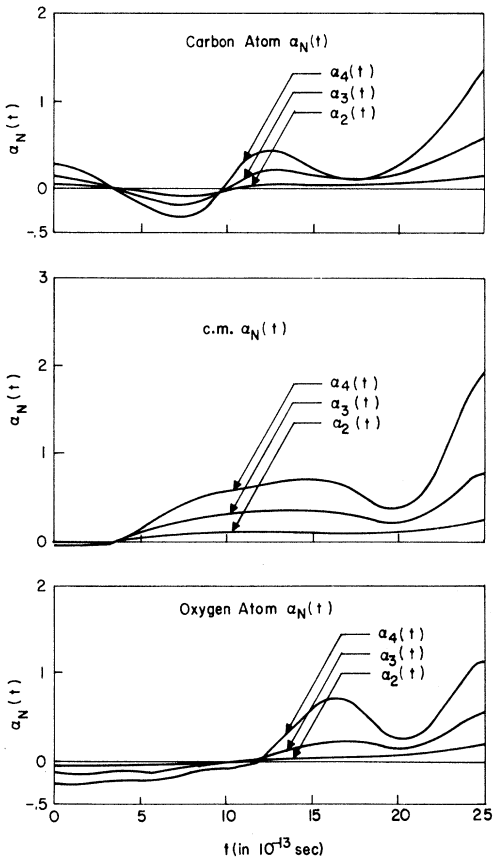

FIG. 24. Non-Gaussian behavior of $G_s^{(\nu)}(r,t)$ in the Stockmayer simulation using 216 molecules.

from the Stockmayer simulation using 216 and 512 molecules, respectively. The corresponding coefficients from the 216 and 512 molecule systems differ substantially from each other. Therefore, we feel that these coefficients from our simulations are only qualitative indications of the non-Gaussian behavior of our self-correlation functions. Figure 26 presents the results from the modified Stockmayer simulation. Comparing the results for the two simulations we see: (1) None of the self-correlation functions is a Gaussian for all time. (2) The self-correlation functions from the Stockmayer simulation are closer to Gaussians than those from the modified Stockmayer simulation. (3) The modified Stockmayer coefficients are always positive in contrast to the Stockmayer coefficients. (4) The Stockmayer coefficients for $G_S(r,t)$ do not vanish for short times.

Finally we conclude this section with a few remarks on the c.m. intermediate scattering function $F_S(\vec{k},t)$. $F_S(\vec{k},t)$ is defined in Table I. Note that $G_S(r,t)$ is formally defined by

$$G_S(\vec{r},t)=\langle\delta(\vec{r}-[\vec{R}_{\text{c.m.}}(t)-\vec{R}_{\text{c.m.}}(0)])\rangle\ .$$

Therefore, $F_S(\vec{k},t)$ is the spatial Fourier transform of $G_S(\vec{r},t)$. In scattering from isotropic systems such as liquids, $F_S(\vec{k},t)$ depends only on the magnitude of $\vec{k}$, i.e., k. For such systems, F_S may also be written as

$$F_S(k,t)=(4\pi/k)\int_0^\infty r\sin kr\,G_S(r,t)\,dr\ .$$

$F_S(k,t)$ from the modified Stockmayer simulation for k equal 2 Å^{-1} and 4 Å^{-1} is presented in Fig. 27. These functions were evaluated using Rahman and Nijboer's[30] series expansion for $F_S(k,t)$ which we also discuss elsewhere.[17] The normalized memory functions for these two intermediate scattering functions are presented in Fig. 28. Note that although the two intermediate scattering functions are quite different, their normalized memories resemble the velocity autocorrelation for this simulation (see Fig. 13). To second order in k it can be shown that

$$\Phi_k(t)=\tfrac{1}{3}k^2\langle V^2\rangle\psi(t)+\theta(k^4)\ .$$

Thus, for sufficiently small values of k, we have

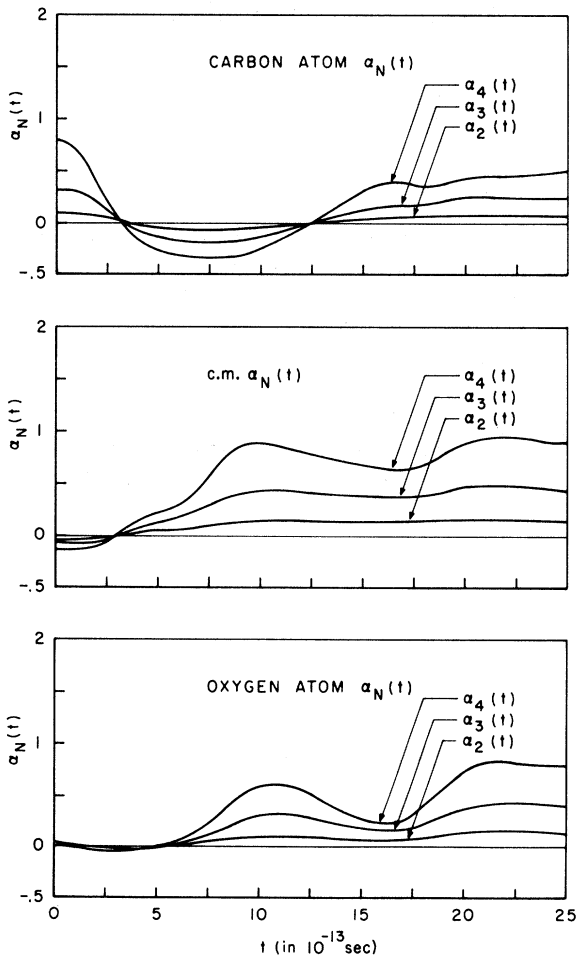

FIG. 25. Non-Gaussian behavior of $G_s^{(\nu)}(r,t)$ in the Stockmayer simulation using 512 molecules.

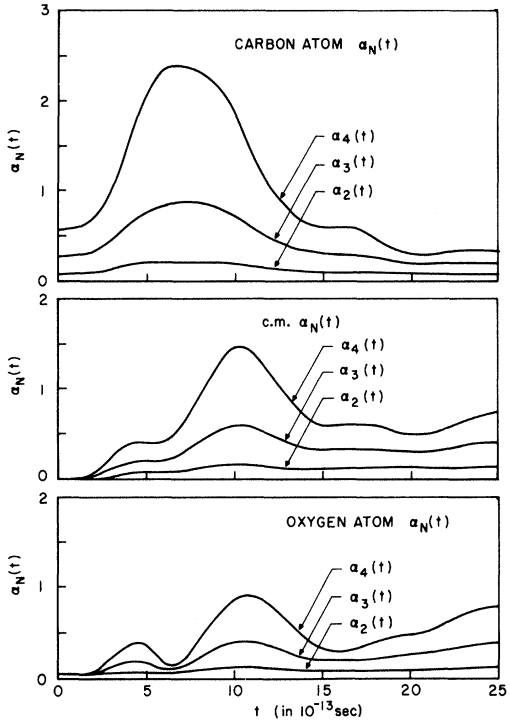

FIG. 26. Non-Gaussian behavior of $G_s^{(\nu)}(r,t)$ in the modified Stockmayer simulation.

$$\Phi_k(t) \simeq \tfrac{1}{3}k^2 \langle V^2 \rangle \psi(t) \ .$$

To get some idea of the values of k for which this expansion is valid look at the second term in the short-time expansion of $\Phi_k(t)$. Note that the term in k^4 can be neglected provided

$$\tfrac{3}{2}\langle a^2 \rangle / \langle V^2 \rangle^2 \gg k^2 \ .$$

In the particular case of the modified Stockmayer simulation the k^4 term can be neglected provided $k \ll 4$ Å^{-1}. The interesting feature of this approximate memory function is that it will lead to a non-Gaussian $G_S(r,t)$ and thus may provide an approximate method for determining $G_S(r,t)$ for intermediate values of k when it is known that $G_S(r,t)$ deviates from a Gaussian. Note that in the Gaussian approximation, $F_S(k,t)$ is given simply by

$$F_S(k,t) = e^{-k^2 \langle [\Delta \vec{R}_{c.m.}(t)]^2 \rangle} \ .$$

The results of using this approximate memory to compute approximate intermediate scattering functions are presented in Fig. 29 along with the corresponding intermediate scattering functions derived from the Gaussian approximation and experiment. Note that the functions derived from the above approximate memory are better than those derived from the Gaussian approximation for intermediate values of k.

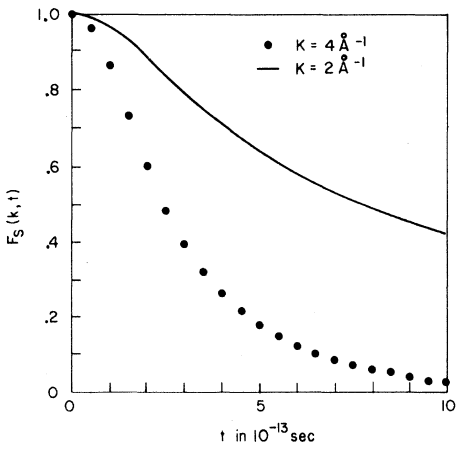

FIG. 27. Intermediate scattering functions for the c. m. from the modified Stockmayer simulation.

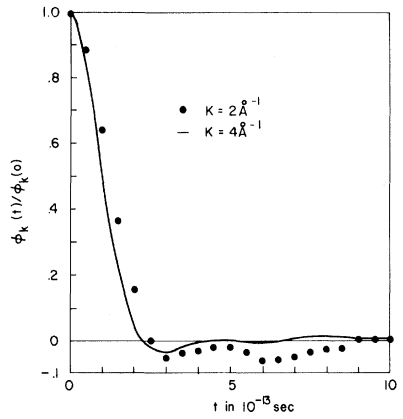

FIG. 28. Intermediate scattering memory functions for the c. m. from the modified Stockmayer simulation.

ACKNOWLEDGMENTS

We would like to thank the staffs of Columbia University's and Brookhaven National Laboratory's computing centers for their cooperation in these calculations.

APPENDIX: MOLECULAR DYNAMICS

The molecular-dynamics calculations were carried out in a manner similar to that used by Rahman[9] in his original study of liquid argon and are described in detail elsewhere.[17,20] We shall primarily be interested in the results from two simulations of liquid carbon monoxide. The first which we shall hereafter refer to as the Stockmayer simulation used a Lennard-Jones plus dipole-dipole pair potential. The small dipole moment of carbon monoxide makes the orientational-dependent part of this potential so weak that molecules from this simulation rotate essentially freely, despite the fact that this calculation was done at a liquid density. The second which we shall hereafter refer to as the modified Stockmayer simulation used a Len-

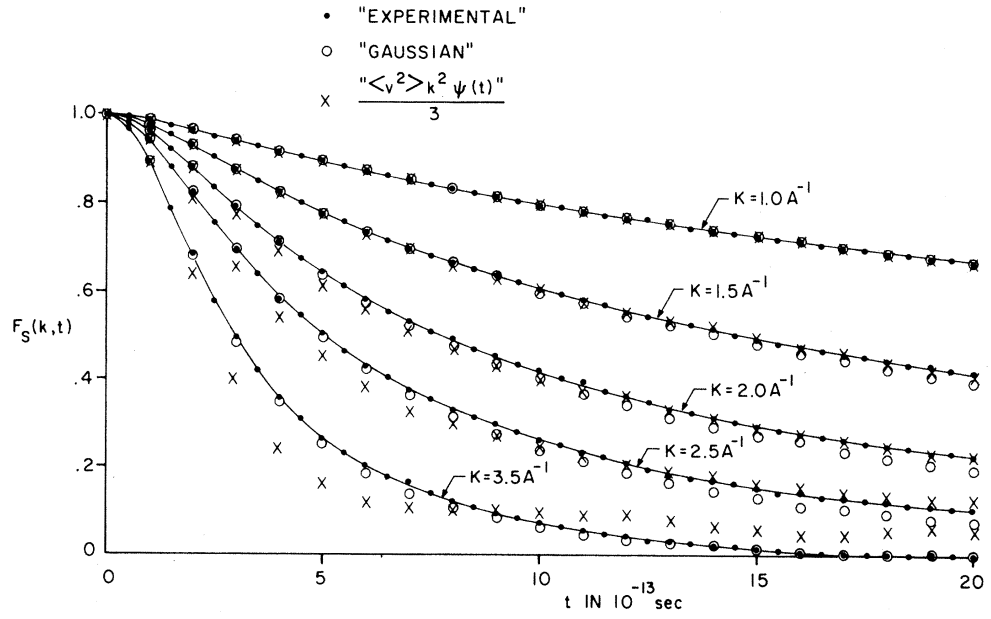

FIG. 29. Intermediate scattering functions for the c. m. from the modified Stockmayer simulation. The approximate scattering functions were calculated using the Gaussian approximation and from the approximation that the memory for $F_s(k,t)$ is given by $\frac{1}{3}k^2\langle v^2\rangle\psi(t)$.

nard Jones plus dipole-dipole, quadrupole-dipole, and quadrupole-quadrupole pair potential. The results from this simulation indicate that this pair potential is slightly stronger than the potential of interaction in real liquid carbon monoxide. For example, the mean-square torque about the c. m. of a molecule is $\sim 36\times10^{-28}$ (dyn cm)^2 for this simulation while the experimental value is $\sim 21\times10^{-28}$(dyn cm)^2.

Both of these simulations were done with 216 and 512 molecules. However, only the results from the simulations using 512 molecules are presented here. Varying the number of molecules used allows one to examine the effects of the periodic boundary conditions on the results.

For the correlation functions discussed here, the primary effect of increasing the number of molecules is to reduce fluctuations in these functions that occur for $t \gtrsim 4\times10^{-13}$ sec. This effect on the velocity autocorrelation function $\psi(t)$ for the Stockmayer simulation is illustrated in Fig. 30.

We have also tried to assess the effects of integrating Hamilton's equations numerically. This is rather a difficult task since the exact solutions to these equations are not known. However, we can use the observed conservation of total energy and linear momentum as an indication that the equations are being integrated properly. For the Stockmayer and modified Stockmayer simulations using 512 molecules the total energy and linear momentum were conserved to ~0.05 and ~0.0006%, respectively, over our entire range of integration.

Correlation functions from molecular-dynamics calculations represent time averages over a finite time interval. However, they are assumed to represent time averages over an infinite interval. For a discussion of the errors that can arise from making such an assumption see Ailawadi[31] and Ailawadi *et al.*[4]

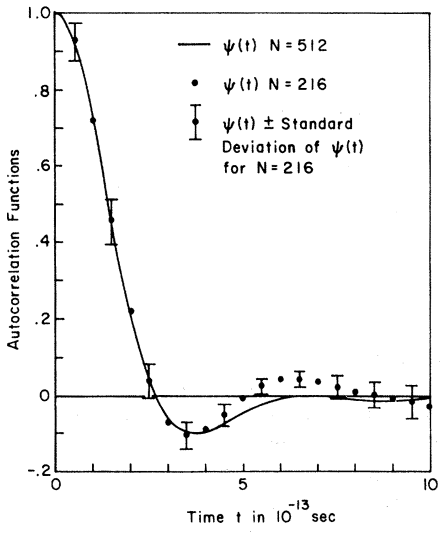

FIG. 30. $\psi(t)$ from the Stockmayer simulation using 216 and 512 molecules.

*Research supported in part by the U. S. Atomic Energy Commission, the National Science Foundation, and the Petroleum Research Foundation of the American Chemical Society.

†Part of research done while this investigator was a National Aeronautics and Space Administration Predoctoral Fellow.

‡Alfred P. Sloan Fellow.

[1]L. Van Hove, Phys. Rev. 95, 249 (1954).

[2]R. Pecora, J. Chem. Phys. 40, 1604 (1964).

[3]R. Mountain, Critical Rev. Solid State Sci. (to be published).

[4]N. Ailawadi, R. Zwanzig, and A. Rahman (to be published).

[5]R. Kubo, *Many Body Theory* (Benjamin, New York, 1966).

[6]R. Gordon, J. Chem. Phys. 44, 1830 (1966).

[7]J. Deutch, J. Kinsey, and R. Silbey, Tech. Report MIT Dept. Chem., 1968 (unpublished); R. Nossal, J. Math. Phys. 6, 193 (1965); J. Kushick and B. J. Berne, Tech. Report Columbia University Dept. Chem., 1969 (unpublished); M. Fixman and K. Rider, J. Chem. Phys. 51, 2425 (1969); J. Lebowitz and J. Percus, Phys. Rev. (to be published).

[8]B. Alder and T. Wainwright, J. Chem. Phys. 31, 459 (1959).

[9]A. Rahman, Phys. Rev. 136, A405 (1964).

[10]L. Verlet, Phys. Rev. 159, 98 (1967).

[11]R. Zwanzig, *Lectures in Theoretical Physics*, edited by W. B. Britlin, W. B. Downs, and J. Downs (Interscience, New York, 1961), Vol. III, p. 106.

[12]H. Mori, Progr. Theoret. Phys. (Kyoto) 33, 423 (1965).

[13]S. Chandrasekhar, Rev. Mod. Phys. 15, 1 (1945).

[14]J. Doob, Ann. Math. 43, 351 (1942).

[15]H. Mori, Progr. Theoret. Phys. (Kyoto) 34, 399 (1965).

[16]W. Feller, *Introduction to Probability Theory and Its Applications*, (Wiley, New York, 1966).

[17]B. J. Berne and G. D. Harp, Advan. Chem. Phys. 17, 63 (1970).

[18]E. T. Jaynes, in *Information Theory and Statistical Mechanics, Statistical Physics*, 1962 *Brandeis Lectures*, edited by K. W. Ford (Benjamin, New York, 1963).

[19]B. J. Alder and T. E. Wainwright, in *Transport Processes in Statistical Mechanics*, edited by I. Prigogine (Interscience, New York, 1958).

[20]G. D. Harp and B. J. Berne, J. Chem. Phys. 49, 1249 (1968).

[21]B. J. Berne, J. P. Boon, and S. A. Rice, J. Chem Phys. 45, 1086 (1966).

[22]K. Singwi and S. Tosi, Phys. Rev. 157, 153 (1967).

[23]B. J. Berne and G. D. Harp, Symposium of AICHE, New York, 1967 (unpublished).

[24]P. Martin and S. Yip, Phys. Rev. 170, 151 (1968).

[25]G. Vineyard, Phys. Rev. 110, 999 (1958).

[26]B. Dasannacharya and K. Rao, Phys. Rev. 137, A417 (1965).

[27]P. A. Egelstaff, *Thermal Neutron Scatterings*, (Academic, London, England, 1965).

[28]B. J. Berne, Ph. D. thesis, University of Chicago, 1964 (unpublished).

[29]R. Desai and S. Yip, Phys. Rev. 166, 129 (1968).

[30]A. Rahman and B. Nijboer, Physica 32, 415 (1966).

[31]N. Ailawadi, Ph. D. thesis, University of Maryland, 1969 (unpublished).

PHYSICAL REVIEW A VOLUME 2, NUMBER 3 SEPTEMBER 1970

Quantum-Mechanical Second Virial Coefficient at High Temperatures

W. G. Gibson

Department of Applied Mathematics, The University of Sydney, New South Wales 2006, *Australia*

(Received 13 March 1970)

An expression is obtained for the quantum-mechanical second virial coefficient in the form of an inverse Laplace transform of the logarithmic derivative of the Jost function. This form is useful for the calculation of the direct part of the virial coefficient at high temperatures in cases where the Wigner-Kirkwood expansion breaks down. Explicit calculations are presented for hard spheres, the square-well potential, and the square-well potential with a hard core.

I. INTRODUCTION

The straightforward method of calculating the direct part of the second virial coefficient at high temperatures uses the Wigner-Kirkwood (WK) expansion.[1] This essentially is a perturbation expansion of the Hamiltonian in powers of the kinetic energy and leads to an expression for the second virial coefficient as a power series in $\hbar^2$. However, for a large class of potentials, the WK expansion breaks down. This class includes all potentials $V(r)$ which are nondifferentiable functions of r, as well as potentials such as the exponential potential for which higher coefficients in the WK expansion diverge. DeWitt[2] has analyzed the quantum corrections to the second virial coefficient for a number of these potentials and has found that they involve nonanalytic forms of $\hbar^2$. The particular case of hard spheres has received some attention,[3-6] and Mohling[5] has also treated the case of a square-well potential with a hard core. In these instances, expansions in powers of $\hbar$ are obtained.

The related problem of calculating the exchange second virial coefficient at high temperatures has